Bronchial inflammation and bacterial load in stable COPD is associated with TLR4 overexpression

(Article begins on next page)

16 October 2023

Bronchial inflammation and bacterial load in stable COPD is associated with TLR4 overexpression

1
2
3
4
5
6
7
8
9
10
11
12
13
14
15
16
17
18
19
20
21
22
23
24
25
26
27
28
29
30
31
32
33
34
35
36
37
38
39
40
41
42
43
44
45
46
47
48
49
50
51
52
53
54
55
56
57
58
59
60

SCHOLARONE™
Manuscripts

1

Bronchial inflammation and bacterial load in stable COPD is associated with TLR4 overexpression

Antonino Di Stefano, PhD[1], Fabio LM Ricciardolo, MD. PhD[2], Gaetano Caramori MD, PhD[3], Ian M Adcock, PhD[4], Kian Fan Chung MD[4], Peter J Barnes MD[4], Paola Brun, PhD[5], Andrea Leonardi, MD[6], Filippo Andò MD[7], Davide Vallese, PhD[1], Isabella Gnemmi[1], Luisella Righi, MD[8], Francesco Cappello, MD[9,10], Bruno Balbi, MD[1]

[1]Divisione di Pneumologia e Laboratorio di Citoimmunopatologia dell'Apparato Cardio Respiratorio, Istituti Clinici Scientifici Maugeri SpA, Società Benefit, Veruno (NO), Italy, [2]Dipartimento di Scienze Cliniche e Biologiche, A.O.U., Divisione di Pneumologia, Ospedale San Luigi, Orbassano, Università di Torino, Italy, [3]Centro Interdipartimentale per lo Studio delle Malattie Infiammatorie delle Vie Aeree e Patologie Fumo-correlate (CEMICEF; formerly named Centro di Ricerca su Asma e BPCO), Sezione di Medicina Interna e Cardiorespiratoria, Università di Ferrara, [4]Airways Disease Section, National Heart and Lung Institute, Imperial College London, UK, [5]Dipartimento di Medicina Molecolare, Università di Padova, Italy, [6]Department of Neuroscience, Ophthalmology Unit, University of Padua, Padua, Italy; [7]UOC di Malattie Respiratorie, Dipartimento di Scienze Biomediche, Odontoiatriche e delle Immagini Morfologiche e Funzionali, Università di Messina, Italy, [8]Dipartimento di Oncologia, SCDU, Anatomia Patologica, A.O.U., San Luigi, Orbassano, Università di Torino, Ospedale San Luigi, Orbassano, Torino, Italy [9]Dipartimento di Biomedicina Sperimentale e Neuroscienze Cliniche, Sezione di Anatomia Umana, Università di Palermo, Italy, [10]Euro-Mediterranean Institute of Science and Technology (IEMEST), Palermo, Italy.

Short title: Inflammation, bacterial load and active anti-bacterial immune response involving TLR4 and NOD1 in stable COPDTLR4 expression in stable COPD

Conflict of interest: No conflict of interest for all the authors included in the present study

Manuscript word count: 30402935

1

1
2
3
4
5   2
6
7   **Correspondence to:**
8
9   Dr Antonino Di Stefano, PhD,
10   Istituti Clinici Scientifici~~Fondazione Salvatore~~ Maugeri, IRCCS,
11
12   Divisione di Pneumologia e Laboratorio di Citoimmunopatologia
13   dell'Apparato Cardio Respiratorio
14   Via per Revislate, 13
15
16   28010 Veruno (NO), Italy
17   tel: +39 0322 884711
18
19   fax: +39 0322 884776
20   E-mail: antonino.distefano@icsmaugeri.it
21
22
23
24
25
26
27
28
29
30
31
32
33
34
35
36
37
38
39
40
41
42
43
44
45
46
47
48
49
50
51
52
53
54
55
56   2
57
58
59
60

3

Abstract

Background: Toll-like receptors (TLRs) and nod-like receptors (NLRs) are two major forms of innate immune sensors but their role in the immunopathology of stable COPD is incompletely studied.

Objectives: To investigate TLRs and NLRs signaling pathways in the bronchial mucosa in stable COPD

Methods: Using immunohistochemistry the expression of TLR2, -4, -9, NOD1, NOD2, CD14, MYD88, TIRAP, pIRAK1, IRAK4 were measured in the bronchial mucosa of subjects with stable COPD of different severity (n=34), control smokers (n=12) and non-smokers (n=12). The bronchial bacterial load of *P. aeruginosa*, *H. influenzae*, *M. catarrhalis*, *S. pneumonie* was measured by qRT-PCR.

Results: TLR4 and NOD1 expression were increased in the bronchial mucosa of patients with severe/very severe stable COPD compared to control subjects. TLR4 bronchial epithelial expression correlated positively with CD4+ and CD8+ cells and the airflow obstruction. NOD1 expression correlated with CD8+ cells. The bronchial load of *P. aeruginosa* was directly correlated, but *H. influenzae* inversely correlated with the degree of airflow obstruction. Bacterial load did not correlate with inflammatory cells.

Conclusions: Bronchial epithelial overexpression of TLR4 and NOD1 in severe/very severe stable COPD, associated with increased bronchial inflammation and *P. aeruginosa* bacterial load, may play a role in the pathogenesis of COPD.

Words count: 200

1
2
3
4
5
6
7
8
9
10
11
12
13
14
15
16
17
18
19
20
21
22
23
24
25
26
27
28
29
30
31
32
33
34
35
36
37
38
39
40
41
42
43
44
45
46
47
48
49
50
51
52
53
54
55
56
57
58
59
60

4

Key words

COPD pathology, bacterial load, innate immune response, toll-like receptors and nod-like receptors

Abbreviations:

FEV_1=forced expiratory volume in one second,

FVC= forced vital capacity.

iE-DAP=γ-D-glutamyl-meso-diaminopimelic acid,

IRAK=IL-1 receptor-associated kinase,

LPS=lipopolysaccharide,

MYD88=myeloid differentiation primary response gene 88,

NOD=nucleotide-binding oligomerization domain,

PAMP=pathogen-associated molecular patterns,

PGN=peptidoglycan,

PRR=pattern-recognition receptors,

TIRAP=TIR domain-containing adaptor protein,

TLR=toll-like receptor,

4

5

Introduction

Inflammation plays a key role in the pathogenesis of chronic obstructive pulmonary disease (COPD) (1). A symbiotic relationship between the microbiota and the innate and adaptive immune host response has been postulated (2, 3). Immune host responses to microbiota challenges are balanced in such a way as to maintain the microbiota diversity required for induction of protective responses to pathogens (2, 3). ~~Chronic obstructive pulmonary disease (COPD) is characterized by an abnormal immune response in the lower airways (1).~~ The innate immune system recognizes microbial pathogens through pattern-recognition receptors (PRRs), which detect the pathogen-associated molecular patterns (PAMPs) and induce inflammatory host responses and activation of the adaptive immune responses (2, 3).

Toll-like receptors (TLRs) and nucleotide-binding oligomerization domain (NOD)-like receptors (NLRs) are two major PRRs~~forms of innate immune sensors~~, which provide responses against pathogenic invasion or tissue injury (4). TLR2 recognizes lipoteichoic acid from Gram positive bacteria and some non-typical lipopolysaccharides (LPS) of Gram negative bacteria (5); TLR4 recognizes LPS and some endogenous ligands (5) and TLR9 is involved in viral A/D- and bacterial B/K-type CpG DNA recognition (6). CD14 acts as a co-receptor (along with TLR4) for the detection of (LPS) but can bind LPS only in the presence of lipopolysaccharide-binding protein (LBP). Although LPS is considered its main ligand, CD14 also recognizes other PAMPs~~pathogen-associated molecular patterns~~ such as lipoteichoic acid (7).

~~Nucleotide-binding oligomerization domain (~~NOD)1 and NOD2 recognize intracellular bacteria through identification of peptidoglycan (PGN) components, such as a muramyl dipeptide (MDP) found in almost all bacteria, or via γ-D-glutamyl-meso-diaminopimelic acid (iE-DAP) found in ~~the~~ Gram-negative bacteria (8). Both myeloid differentiation primary response gene 88 (MYD88)-dependent and -independent (involving the CD14) signaling

5

Formatted: Font: (Default) Arial

Formatted: Font: (Default) Arial
Formatted: Font: (Default) Arial
Formatted: Font: (Default) Arial
Formatted: Font: (Default) Arial
Formatted: Font: (Default) Arial

Formatted: Font: (Default) Arial
Formatted: Font: (Default) Arial
Formatted: Font: (Default) Arial

6

pathways are activated downstream of TLR activation (9, 10). Upon receptor stimulation, MYD88 recruits interleukin-1 receptor-associated kinase (IRAK)-4 to TLRs and induces IRAK-1 phosphorylation, followed, in turn, by AP-1 activation and nuclear translocation and/or IκB degradation and NF-κB nuclear activation (11-14). TIR domain-containing adaptor protein (TIRAP) is essential for the MYD88-dependent signaling pathway through TLR2 and TLR4 activation (15).

Abnormalities in any of these innate sensor-mediated processes may result in excessive inflammation due to either hyperactive innate immune signaling or sustained compensatory adaptive immune activation (4, 5). These characteristics have been observed in the lower airways of patients with stable COPD (1). We hypothesize the detection of bacterial proteins occursis activated to a greater extent in more severe COPD. The aim of this study was to investigate TLRs and NLRs signaling pathways in the bronchial mucosa in relation to the bronchial bacterial load of patients with stable COPD of differing severity and control subjects.

6

7

Methods

Subjects

All COPD patients and control subjects who underwent bronchoscopy and bronchial biopsies were recruited from the Respiratory Medicine Unit of the Fondazione Salvatore Maugeri, Institute of Veruno (Veruno, Italy). In COPD patients, the severity of the airflow obstruction was graded using current GOLD criteria [http://goldcopd.org/]. All former smokers had stopped smoking for at least one year. COPD and chronic bronchitis were defined, according to international guidelines, [http://goldcopd.org/]. All COPD patients were stable with no exacerbation in the six months prior to bronchoscopy. None of the subjects was treated with theophylline, antibiotics, antioxidants, mucolytics, and/or glucocorticoids in the month prior bronchoscopy. The study conformed to the Declaration of Helsinki and was approved by the ethics committees of the Fondazione Salvatore Maugeri [Veruno (Novara), Italy], the University Hospital of Ferrara, Italy. Written informed consent was obtained from each subject and bronchial biopsies were performed according to the local ethic committee guidelines.

A detailed description of subjects, lung function tests, fibreoptic bronchoscopy and processing of bronchial biopsies, immunohistochemistry, scoring system for immunohistochemistry, double staining, quantification of bacterial load and "*in vitro*"

> **Formatted:** Font: Italic

experiments performed on normal human bronchial epithelial (NHBE) cells and details of statistical analysis are provided in the supplementary material.

Statistical analysis

The numbers of patients used in each group was based on previous studies which examined differences in inflammatory cell numbers in bronchial biopsies (16). Differences between groups were analyzed using analysis of variance (ANOVA) for functional data. The ANOVA test was followed by the unpaired t-test for comparison between groups. The

8

~~Kruskal-Wallis test applied for morphologic data was followed by the Mann-Whitney U test for comparison between groups. Correlation coefficients were calculated using the Spearman rank method. Probability values of $p < 0.05$ were considered significant.~~Differences between groups were analysed using analysis of variance and Kruskal-Wallis tests. Correlation coefficients were calculated using the Spearman rank method.

Formatted: Justified

8

9

Results

Clinical characteristics of the subjects

We obtained and studied bronchial biopsies from 58 subjects: 34 with stable COPD, 12 control smokers with normal lung function, and 12 non-smokers with normal lung function (**Table 1**). COPD patients were divided into two groups: mild/moderate (GOLD stage I-II, n=16) and severe/very severe GOLD stage III-IV, n=18) [www.goldcopd.org]. There was no difference in age between the subjects in the all four groups. The smoking history was similar in the three smoking groups. Values of FEV_1 (% predicted) and FEV_1/FVC (%) differed significantly between total COPD patients (mild/moderate and severe/very severe) and both control groups (healthy smokers and healthy non-smokers). Lung function in severe/very severe COPD patients also differed significantly from mild/moderate COPD patients (ANOVA: $p<0.0001$ for FEV_1% predicted and FEV_1/FVC% values). Thirty-five percent (n=12) of the total COPD patients and 25% (n=3) of healthy smokers with normal lung function also had symptoms of chronic bronchitis but this was not significantly.

Inflammatory cells in the bronchial biopsies

The results of the immunohistochemical analysisstudy are summarised in **Table 2**. These data, obtained from stable COPD patients by immunohistochemistry, confirm previously reported results showing higher numbers of neutrophils in severe/very severe COPD (**Table 2**) (16). There was also a trend towards increased CD8+ cell numbers in severe and very severe patients but this did not reach significance according to the Kruskal-Wallis test. COPD patients with chronic bronchitis had a similar number of neutrophils when compared with COPD patients without chronic bronchitis (16, 17).

Immunohistochemistry for the TLRs and NLRs signaling pathways in the bronchial biopsies

9

Formatted: No widow/orphan control

10

The results of the immunohistochemical study for the TLRs and NLRs signaling pathways are summarized in **Table 2**.

Immunohistochemistry ~~for the TLRs and NLRs signaling pathways~~ in ~~the~~ bronchial epithelium

The expression of TLR4 in the bronchial epithelium was increased in severe/very severe stable COPD compared to non-smoking control subjects (p=0.0027) (**Table 2, Figure E1**). There was a trend towards significance between these COPD patients and control smokers with normal lung function (p=0.054). The expression of TLR4 in the bronchial epithelium was also increased in mild/moderate stable COPD patients compared with non-smoking control subjects (p=0.024). Similarly, the expression of NOD1 in the bronchial epithelium was increased in severe/very severe stable COPD compared to mild/moderate stable COPD patients (p=0.036) and non-smoking control subjects (p=0.006) (**Table 2, Figure E2**). NOD1 expression also trended towards significance between severe/very severe stable COPD patients and control smokers with normal lung function (p=0.054).

The bronchial epithelial~~um~~ expression of both MYD88 (Kruskal-Wallis:p=0.059, Mann-Whitney:p=0.012 and p=0.038, respectively) and TIRAP (Kruskal-Wallis:p=0.082, Mann-Whitney:p=0.035 and p=0.047, respectively) also tended to be increased in severe/very severe stable COPD patients compared to mild/moderate COPD and control smokers with normal lung function (**Table 2**). No significant differences were observed for the other molecules studied (**Table 2**). These data are also summarized in **Figure 1A**.

Immunohistochemistry ~~for the TLRs and NLRs signaling pathways~~ in ~~the~~ bronchial lamina propria

TLR4 was increased in severe/very severe COPD (p=0.027) and mild/moderate COPD (p=0.015) compared to control smokers (**Table 2, Figure E1**). NOD1 was increased in

10

11

severe/very severe COPD compared to control smokers (p=0.022) and control non-smokers (p=0.002). It was also increased in mild/moderate COPD (p=0.023) compared to control non-smokers (**Table 2, Figure E2**). IRAK4 tended to be increased in mild/moderate COPD (Kruskal-Wallis: p=0.071, Mann Whitney: p=0.017) compared to control smokers (**Table 2**). No statistical differences were observed for the other molecules studied (**Table 2**). These data are summarized in **Figure 1B**. Double staining for identification of CD8+ (T-cell), CD68+ (macrophage) and CD31+ (endothelial) cells co-expressing TLR4 and NOD1 was performed in three representative COPD patients. The percentage of (mean±s.e.) CD8+ TLR4+, CD68+TLR4+ and CD31+TLR4+ double stained cells were 51±11%, 54±12% and 61±5%, respectively; the percentage of CD8+ NOD1+, CD68+NOD1+ and CD31+NOD1+ double stained cells were 31±10%, 30±5% and 43±5%, respectively (**Figure E3**).

Quantification of bacterial load in the bronchial biopsies

The results of the quantification of the bacterial load in bronchial biopsies are summarized in **Table 3** and **Figure 1C**. When data were expressed as absolute numbers, *H. influenzae* was decreased in severe/very severe COPD compared to mild/moderate COPD (p=0.011) and control smokers (p=0.0013). No significant differences were observed for *P. aeruginosa*, *M. catarrhalis* and *S. pneumoniae* (**Table 3**). To evaluate changes on the relative proportions of each bacterium studied, we expressed these data as percentage of the total load value constituted by the sum of the four bacteria studied. The percentage of *P. aeruginosa* tended to be increased in severe/very severe stable COPD compared to control smokers with normal lung function (Kruskal Wallis: p=0.050, Mann-Whitney: p=0.012); the percentage of H. *influenzae* was significantly decreased in severe/very severe COPD compared to mild/moderate COPD (p=0.029) and control smokers (p=0.010) (**Table 3, Figure 1C**).

11

12

Quantification of TLR4 mRNA in "in vitro" H_2O_2 treated bronchial epithelial cells.

Bronchial epithelial (16HBE) cells treated with H_2O_2 (100µM) showed significantly increased TLR4 mRNA levels after 2h (**Figure 1D**).

Correlations between clinical parameters, number of inflammatory cells, TLRs and NLRs signaling pathways expression and bacterial load in the bronchial biopsies

In all smokers, the degree of TLR4 immunostaining in the bronchial epithelium was positively correlated with the numbers of CD8+ cells (r=0.630, p=0.018) and CD4+ cells (r=0.580, p=0.029) in the bronchial lamina propria. In addition, in all smokers, the degree of TLR4 immunostaining in bronchial epithelium was inversely correlated with the $FEV_1\%$ of the predicted (r=-0.36, p=0.019) and the $FEV_1/FVC\%$ (r=-0.39, p=0.009). When the analysis was restricted to patients with stable COPD alone, the correlations between the degree of TLR4 immunostaining in the bronchial epithelium with FEV1% predicted (r=-0.37, p=0.037) and FEV_1/FVC ratio (r=-0.50, p=0.005) was maintained (**Figure 2**). In all smokers, NOD1 immunostaining in the lamina propria was inversely correlated with the $FEV_1\%$ predicted values (r=-0.39, p=0.019) and positively correlated with the numbers of CD8+ cells (r= 0.538, p=0.044).

Interestingly, in all smokers, the bronchial load of *P. aeruginosa* was inversely correlated with the $FEV_1\%$ of the predicted values (r=-0.41, p=0.012) (**Figure 3**); whereas the reverse effect was seen with the bronchial load of *H. influenzae* which was positively correlated with the $FEV_1\%$ of the predicted (r=0.458, p=0.005) (**Figure 3**). This association was ~~also~~ maintained in the COPD patient group when studied separately (r=0.424, p=0.025).

No other statistically significant correlations were found between clinical parameters, expression of bacterial receptors, number of inflammatory cells and bacterial load.

12

1
2
3
4
5
6
7
8
9
10
11
12
13
14
15
16
17
18
19
20
21
22
23
24
25
26
27
28
29
30
31
32
33
34
35
36
37
38
39
40
41
42
43
44
45
46
47
48
49
50
51
52
53
54
55
56
57
58
59
60

13

13

14

Discussion

We have shown here that TLR4 and NOD1 protein expression is enhanced in the bronchial mucosa of patients with severe/very severe COPD compared to control subjects. In addition the bronchial epithelial expression of TLR4 correlates positively with the numbers of CD4+ and CD8+ cells in the bronchial mucosa and with the degree of airflow obstruction. NOD1 expression also correlated with CD8+ cell numbers. The degree of airflow obstruction was positively correlated with an increased load of *P. aeruginosa* and a decreased load of *H. influenzae* in the bronchial biopsies in all smokers and in patients with stable COPD.

A previous study ~~has~~ found no significant differences in TLR4 expression in the bronchial mucosa ~~l expression of TLR4~~ of mild/moderate stable COPD patients compared to control subjects, while the percentage of CD8+ cells co-expressing TLR4 was increased (18). The difference between ~~with~~ the results reported here could be due to the low number of COPD ~~patients~~ (n=8) and control subjects (n=5) studied (18) and also due to the different severity of ~~their~~ the COPD patients. In all smokers and patients with COPD, we found a significant positive correlation between TLR4 epithelial expression and numbers of CD8+ and CD4+ cells in the lamina propria, showing an association between bronchial inflammation and upregulation of TLR4 in stable COPD. Furthermore, in agreement with our present data, increased TLR4 expression was reported by Western blotting in GOLD stage 4 COPD patients compared to control non-smokers (19). In contrast, Lee and colleagues reported decreased TLR4 levels associated with increased bronchial obstruction and increased emphysema score on lung lysates of smokers (20) confirming the need for further investigations to correctly position our present data. We here showed that CD8+, CD68+ and CD31+ cells mainly contributed to the up-regulation of TLR4 and NOD1 in bronchial biopsies of COPD patients. In agreement, using flow

14

15

cytometric analysis, CD8+ cells co-expressing TLR4 were also increased in the peripheral lung tissue of COPD patients compared to control smokers (21).

TLR4 recognises lipopolysaccharides (LPS), the major surface component of Gram-negative bacteria (5). Lipid A is the pro-inflammatory component of LPS and TLR4 is required for the recognition of lipid A of *P. aeruginosa* (22) suggesting that its overexpression in the bronchial epithelium of severe/very severe stable COPD patients may be important for sensing and responding to persistent colonization of the lower airways of these patients (23). Interestingly, *in vitro,* TLR4 activates NF-κB and propagate and maintain oxidative/nitrosative cellular stress that are both involved in the pathogenesis of stable COPD (1, 24).

Oxidative stress is more pronounced in advanced COPD (1) and *in vitro* both tobacco smoking exposure (18) and oxidative stress (25) may upregulate TLR4 expression. In our *in vitro* experiments, using human bronchial epithelial cells (16HBE) treated with H_2O_2, we showed that oxidative stress induced TLR4 mRNA. Recent evidence in smoking mice (26) indicates that cigarette smoke significantly enhanced *tlr4* mRNA expression after 4 (1.77 fold) and 12 weeks (1.53 fold). Furthermore, ozone enhanced *tlr4* mRNA in the lungs of mice after 6 weeks of exposure is completely ablated by treatment with N-acetylcysteine (unpublished data). This data, taken together, ~~may~~ indicates that increased oxidative stress ~~in COPD patients~~ could be~~is~~ capable of up-regulating TLR4 also in the bronchi of stable COPD patients, a~~leven~~though specific studies in humans need to be performed to confirm this hypothesis.~~.~~

We also demonstrated ~~here for the first time, an~~ increased expression of NOD1 in bronchial epithelium and lamina propria of stable COPD patients compared to control subjects, suggesting an involvement of this cytosolic protein in the recognition process of bacterial cell wall components in the bronchial mucosa of patients with stable COPD (27). *In vitro* human bronchial epithelial cells challenged with *M. catarrhalis* show an increased

15

16

CXCL-8 expression that is blocked by NOD1 inhibitors (28). In addition, *in vitro* NOD1 agonists activates NF-κB in human endothelial cells (29), supporting the role of NOD1 in sustaining bronchial inflammation.

The increased expression of MYD88 in the bronchial epithelium of patients with severe/very severe stable COPD compared to control smokers with normal lung function, without significant differences in CD14 expression, suggests the involvement of a MYD88-dependent downstream signaling pathway in the immunopathology of the bronchial mucosa of stable COPD patients. This is in keeping with our data showing a tendentially increased expression of TIRAP in the bronchial epithelium of our severe/very severe COPD patients, an index of MYD88-dependent pathway activation (15) **(Figures 1 and 4**).

The decreased *H. influenzae* load observed in the bronchial mucosa of our patients with severe/very severe stable COPD compared to mild/moderate COPD and control smokers with normal lung function is in keeping with previous studies showing a fundamental role of TLR4 activation in the clearance of this bacteria from the mouse lung (30, 31). This is also in agreement with previous studies showing that *H. influenzae* is virtually absent in severe/very severe COPD lung tissues and increased in milder forms of COPD (32). The absence of *H. influenzae* may also provide a niche for colonization by other pathogenic bacteria such as new strains of *P. aeurginosa* (32, 33).

Our data on the bronchial bacterial load are only apparently discordant with a previous study performed in the lung parenchymal tissues. This showeding no significant differences in total bacterial load between advanced stable COPD and control subjects (34) and may reflect . This may be due to the different lower airway compartments of the lower airways examined. In fact, Pprevious studies have clearly demonstrated a progressive decrease of the total bacterial load from upper to lower airways and lung parenchyma (32, 33, 35), and this makes more difficult to identify significant differences between patients with stable COPD of different severities and control subjects in the

16

Formatted: Font: Italic

17

presence of very low levels of total bacterial load. This difference may also influence the related immune host response developing in the bronchi and lung tissue (different compartments) of COPD patients when compared to control subjects. These considerations are also reinforced by the data of Cabrera-Rubio et al. (36) showing that in patients with stable COPD the microbiota composition obtained by the analysis of bronchial biopsies and bronchoalveolar lavage better represents the lower airway bacterial composition compared to the analysis of sputum and bronchial aspirate samples (36).

Neither *P. aeruginosa* nor *H. influenzae,* expressed as absolute number or as percentage, were correlated with inflammatory cells (CD8+, CD68+ neutrophils) or bacterial-related molecules (TLR4, NOD1) mainly expressed in the bronchial biopsies. This finding suggests that in stable disease the microbiota may not be directly related to the classical COPD inflammatory response developing in the bronchial mucosa. This seems to be in contrast to the situation during COPD exacerbations where a concomitant increase of bronchial inflammation (37), microbiota load (38) and TLR4 expression (39) has been observed. However, a comprehensive study of pathogen-related bacteria and related inflammatory response in bronchial biopsies of exacerbated COPD patients is lacking. Furthermore, changes in microbial composition in the lung and gut have been linked to organ-related alterations of the immune responses. However, no studies have investigated changes in the gut microbiota of patients with COPD of increasing severity (40).

It is interesting to note that certain single nucleotide polymorphisms (SNPs) of the NOD2 gene were associated with more severe disease in Japanese COPD patients (410) and this area deserves more research in the future. Furthermore, in our current present study, the expression of both IRAK4 and pIRAK1, which favorfavoring NF-κB nuclear activation (11), were both over well expressed in the bronchial epithelium and lamina propria of all subjects studied. This indicates , suggesting that the bronchial mucosa is

18

activated ~~an active state of the bronchial mucosa, even~~ in COPD ~~the absence of significant quantitative differences between COPD patients and control groups~~ (**Figures 1 and 4**). A more expansive study using next generation sequencing may determine the precise differences in inflammation and immunity in these patients.

As a limitation of this study, and in agreement with other authors (33), we cannot exclude a bias in the quantification of the bacterial load due to repeated antibiotic treatments, particularly in severe/very severe COPD patients, even though a one-month wash-out period from antibiotic treatments was applied in our protocol study. In addition, the study was not powered to detect the effect of smoking cessation on these parameters and further larger studies are required to confirm these data as well as the subgroup analysis performed here.

In conclusion, the overexpression of TLR4 and NOD1 in the bronchial epithelium of patients with severe/very severe stable COPD, associated to increased bronchial inflammation and *P. aeruginosa* bacterial load may play a role in the pathogenesis of the disease.

1
2
3
4
5
6
7
8
9
10
11
12
13
14
15
16
17
18
19
20
21
22
23
24
25
26
27
28
29
30
31
32
33
34
35
36
37
38
39
40
41
42
43
44
45
46
47
48
49
50
51
52
53
54
55
56
57
58
59
60

19

19

20

References

1. **Barnes PJ.** Cellular and molecular mechanisms of chronic obstructive pulmonary disease. Clin Chest Med. 2014;35:71-86.

2. **Belkaid Y, Hand TW.** Role of the microbiota in immunity and inflammation. Cell. 2014;157:121-141.

3. **Iwasaki A, Medzhitov R.** Control of adaptive immunity by the innate immune system. Nat Immunol. 2015;16:343-353.

4. **Fukata M, Vamadevan AS, Abreu MT.** Toll-like receptors (TLRs) and Nod-like receptors (NLRs) in inflammatory disorders. Semin Immunol. 2009;21:242-53.

5. **Takeda K, Akira S.** Toll-like receptors in innate immunity. Int Immunol. 2005;17:1-14.

6. **Lund J, Sato A, Akira S, Medzhitov R, Iwasaki A.** Toll-like receptor 9-mediated recognition of Herpes simplex virus-2 by plasmacytoid dendritic cells. J Exp Med. 2003;198:513-520.

7. **Ranoa DR, Kelley SL, Tapping RI.** Human lipopolysaccharide-binding protein (LBP) and CD14 independently deliver triacylated lipoproteins to Toll-like receptor 1 (TLR1) and TLR2 and enhance formation of the ternary signaling complex. J Biol Chem. 2013;288:9729-41.

8. **Girardin SE, Boneca IG, Viala J, Chamaillard M, Labigne A, Thomas G, Philpott DJ, Sansonetti PJ.** Nod2 is a general sensor of peptidoglycan through muramyl dipeptide (MDP) detection. J Biol Chem. 2003;278:8869-8872.

9. **Hemmi H**, **Kaisho T**, **Takeda K**, **Akira S**. The roles of Toll-like receptor 9, MyD88, and DNA-dependent protein kinase catalytic subunit in the effects of two distinct CpG DNAs on dendritic cell subsets. J Immunol. 2003;170:3059-3064.

10. **Ito T, Amakawa R, Kaisho T, Hemmi H, Tajima K, Uehira K, Ozaki Y, Tomizawa H, Akira S, Fukuhara S**. Interferon-alpha and interleukin-12 are induced differentially by Toll-

20

21

like receptor 7 ligands in human blood dendritic cell subsets. J Exp Med. 2002;195:1507-1512.

11. **Takeuchi O**, **Takeda K**, **Hoshino K, Adachi O, Ogawa T, Akira S.** Cellular responses to bacterial cell wall components are mediated through MyD88-dependent signaling cascades. Int Immunol. 2000;12:113-117.

12. **Kawai T, Adachi O, Ogawa T, Takeda K, Akira S.** Unresponsiveness of MyD88-deficient mice to endotoxin. Immunity. 1999;11:115-122.

13. **Schnare M, Holt AC, Takeda K, Akira S, Medzhitov R.** Recognition of CpG DNA is mediated by signaling pathways dependent on the adaptor protein MyD88. Curr Biol. 2000;10:1139-1142.

14. **Häcker H, Vabulas RM, Takeuchi O, Hoshino K, Akira S, Wagner H.** Immune cell activation by bacterial CpG-DNA through myeloid differentiation marker 88 and tumor necrosis factor receptor-associated factor (TRAF)6. J Exp Med. 2000;192:595-600.

15. **Yamamoto M**, **Sato S**, **Hemmi H**, **Sanjo H, Uematsu S, Kaisho T, Hoshino K, Takeuchi O, Kobayashi M, Fujita T, Takeda K, Akira S.** Essential role for TIRAP in activation of the signalling cascade shared by TLR2 and TLR4. Nature. 2002;420:324-329.

16. **Di Stefano A, Caramori G, Barczyk A, Vicari C, Brun P, Zanini A, Cappello F, Garofano E, Padovani A, Contoli M, Casolari P, Durham AL, Chung KF, Barnes PJ, Papi A, Adcock I, Balbi B.** Innate immunity but not NLRP3 inflammasome activation correlates with severity of stable COPD. Thorax. 2014;69:516-524.

17. **Vallese D, Ricciardolo FL, Gnemmi I, Casolari P, Brun P, Sorbello V, Capelli A, Cappello F, Cavallesco GN, Papi A, Chung KF, Balbi B, Adcock IM, Caramori G, Di Stefano A.** Phospho-p38 MAPK expression in COPD patients and asthmatics and in challenged bronchial epithelium. Respiration. 2015;89:329-342.

18. **Nadigel J, Préfontaine D, Baglole CJ, Maltais F, Bourbeau J, Eidelman DH, Hamid Q.** Cigarette smoke increases TLR4 and TLR9 expression and induces cytokine

21

22

production from CD8(+) T cells in chronic obstructive pulmonary disease. Respir Res. 2011;12:149. doi: 10.1186/1465-9921-12-149.

19. **An CH, Wang XM, Lam HC, Ifedigbo E, Washko GR, Ryter SW, Choi AM.** TLR4 deficiency promotes autophagy during cigarette smoke-induced pulmonary emphysema. Am J Physiol Lung Cell Mol Physiol. 2012 Nov 1;303(9):L748-57.

20. **Lee SW, Kim DR, Kim TJ, Paik JH, Chung JH, Jheon S, Huh JW, Lee JH, Lee CT.** The association of down-regulated toll-like receptor 4 expression with airflow limitation and emphysema in smokers. Respir Res. 2012 Nov 21;13:106.

21. **Freeman CM, Martinez FJ, Han MK, Washko GR Jr, McCubbrey AL, Chensue SW, Arenberg DA, Meldrum CA, McCloskey L, Curtis JL.** Lung CD8+ T cells in COPD have increased expression of bacterial TLRs. Respir Res. 2013 Feb 1;14:13.

22. **Ernst RK, Hajjar AM, Tsai JH, Moskowitz SM, Wilson CB, Miller SI.** Pseudomonas aeruginosa lipid A diversity and its recognition by Toll-like receptor 4. J Endotoxin Res. 2003;9:395-400.

23. **Gallego M, Pomares X, Espasa M, Castañer E, Solé M, Suárez D, Monsó E, Montón C.** Pseudomonas aeruginosa isolates in severe chronic obstructive pulmonary disease: characterization and risk factors. BMC Pulm Med. 2014;14:103. doi: 10.1186/1471-2466-14-103.

24. **Karki R**, **Igwe OJ.** Toll-like receptor 4-mediated nuclear factor kappa B activation is essential for sensing exogenous oxidants to propagate and maintain oxidative/nitrosative cellular stress. PLoS One. 2013;8:e73840. doi: 10.1371/journal.pone.0073840. eCollection 2013.

25. **Lucas K, Maes M.** Role of the Toll Like receptor (TLR) radical cycle in chronic inflammation: possible treatments targeting the TLR4 pathway. Mol Neurobiol. 2013;48:190-204. doi: 10.1007/s12035-013-8425-7.

22

23

26. **Haw TJ, Starkey MR Pavlidis S, Nair PM, Liu G, Hanish I,. Kim RY, Foster PS, Adcock IM, Horvat JC, Hansbro PM.** TLR2 and TLR4 have Opposing Roles in the Pathogenesis of Cigarette Smoke-induced COPD Am J Respir Cell Mol Biol 2016 (in press).

27. **Leissinger M, Kulkarni R, Zemans RL, Downey GP, Jeyaseelan S**. Investigating the role of nucleotide-binding oligomerization domain-like receptors in bacterial lung infection. Am J Respir Crit Care Med. 2014;189:1461-1468.

28. **Slevogt H**, **Seybold J**, **Tiwari KN, Hocke AC, Jonatat C, Dietel S, Hippenstiel S, Singer BB, Bachmann S, Suttorp N, Opitz B.** Moraxella catarrhalis is internalized in respiratory epithelial cells by a trigger-like mechanism and initiates a TLR2- and partly NOD1-dependent inflammatory immune response. Cell Microbiol. 2007;9:694-707.

29. **Gatheral T, Reed DM, Moreno L, Gough PJ, Votta BJ, Sehon CA, Rickard DJ, Bertin J, Lim E, Nicholson AG, Mitchell JA.** A key role for the endothelium in NOD1 mediated vascular inflammation: comparison to TLR4 responses. PLoS One. 2012;7:e42386.

30. **Wang X, Moser C, Louboutin JP, Lysenko ES, Weiner DJ, Weiser JN, Wilson JM.** Toll-like receptor 4 mediates innate immune responses to Haemophilus influenzae infection in mouse lung. J Immunol. 2002;168:810-815.

31. **Wieland CW, Florquin S, Maris NA, Hoebe K, Beutler B, Takeda K, Akira S, van der Poll T**. The MyD88-dependent, but not the MyD88-independent, pathway of TLR4 signaling is important in clearing nontypeable haemophilus influenzae from the mouse lung. J Immunol. 2005;175:6042-6049.

32. **Sze MA, Dimitriu PA, Suzuki M, McDonough JE, Campbell JD, Brothers JF, Erb-Downward JR, Huffnagle GB, Hayashi S, Elliott WM, Cooper J, Sin DD, Lenburg ME,**

23

24

Spira A, Mohn WW, Hogg JC. Host Response to the Lung Microbiome in Chronic Obstructive Pulmonary Disease. Am J Respir Crit Care Med. 2015;192:438-445.

33. **Dickson RP, Erb-Downward JR, Huffnagle GB.** Homeostasis and its disruption in the lung microbiome. Am J Physiol Lung Cell Mol Physiol. 2015;309:L1047-1055.

34. **Sze MA, Dimitriu PA, Hayashi S, Elliott WM, McDonough JE, Gosselink JV, Cooper J, Sin DD, Mohn WW, Hogg JC.** The lung tissue microbiome in chronic obstructive pulmonary disease. Am J Respir Crit Care Med. 2012;185:1073-1080.

35. **Charlson ES, Bittinger K, Haas AR, Fitzgerald AS, Frank I, Yadav A, Bushman FD, Collman RG.** Topographical continuity of bacterial populations in the healthy human respiratory tract. Am J Respir Crit Care Med. 2011;184:957-963.

36. **Cabrera-Rubio R, Garcia-Núñez M, Setó L, Antó JM, Moya A, Monsó E, Mira A.** Microbiome diversity in the bronchial tracts of patients with chronic obstructive pulmonary disease J Clin Microbiol. 2012;50:3562-3568.

37. **Saetta M, Di Stefano A, Maestrelli P, Turato G, Ruggieri MP, Roggeri A, Calcagni P, Mapp CE, Ciaccia A, Fabbri LM.** Airway eosinophilia in chronic bronchitis during exacerbations. Am J Respir Crit Care Med. 1994;150:1646-52.

38. **D'Anna SE, Balbi B, Cappello F, Carone M, Di Stefano A.** Bacterial-viral load and the immune response in stable and exacerbated COPD: significance and therapeutic prospects. Int J Chron Obstruct Pulmon Dis. 2016;11:445-453.

39. **Pace E, Ferraro M, Giarratano A, Cipollina C, Gjomarkaj M.** TLR4 up-regulation and reduced Foxp3 expression in mechanically ventilated smokers with obstructive chronic bronchitis. COPD. 2013 Apr;10(2):147-55.

40. **Budden KF, Gellatly SL, Wood DL, Cooper MA, Morrison M, Hugenholtz P, Hansbro PM.** Emerging pathogenic links between microbiota and the gut-lung axis. Nat Rev Microbiol. 2017; 15(1):55-63. doi: 10.1038/nrmicro.2016.142. Epub 2016 Oct 3.

24

25

41. **Kinose D, Ogawa E, Hirota T, Ito I, Kudo M, Haruna A, Marumo S, Hoshino Y, Muro S, Hirai T, Sakai H, Date H, Tamari M, Mishima M**. A NOD2 gene polymorphism is associated with the prevalence and severity of chronic obstructive pulmonary disease in a Japanese population. Respirology. 2012;17:164-171.

Formatted: Font: Italian (Italy)

25

26

Tables

Table 1. Clinical characteristics of COPD and control subjects who provided bronchial biopsies

Groups	n	Age (years)	M/F	Pack years	Ex/current smokers	FEV$_1$ (%pred) pre-β_2	FEV$_1$ (%pred) Post-β_2	FEV$_1$/FVC (%)
Control non-smokers	12	63±13	10/2	0	0	117±18	ND	86±10
Control smokers with normal lung function	12	61±7	9/3	43±26	2/10	104±13	ND	81±6
COPD stages I and II (mild/moderate)	16	71±8	14/3	50±28	6/11	63±11[#]	67±13	57±9[#]
COPD stages III and IV (severe/very severe)	18	66±9	11/7	54±36	13/5	35±8[#&]	38±9	44±10[#&]

Patients were classified according to GOLD (http://goldcopd.org) levels of severity for COPD into: mild (stage I), moderate (stage II), severe (stage III), and very severe (stage IV). Data are mean±SD. For COPD patients FEV$_1$/FVC (%) are post-bronchodilator values. Abbreviations: M, male; F, female, FEV$_1$: forced expiratory volume in one second; FVC, forced vital capacity; ND, not determined; COPD, chronic obstructive pulmonary disease. Statistics. (ANOVA) [#]p<0.0001, significantly different from control smokers with normal lung function and control never-smokers; [&]p<0.0001, significantly different from mild/moderate COPD: (ANOVA)

26

27

Table 2. Immunohistochemical quantification of innate immune molecules and cytokines related to bacterial response in bronchial biopsies

	Control non Smokers	Control Smokers	Mild/Moderate COPD	Severe/very Severe COPD	Kruskal Wallis p value
Epithelium (score 0-3)					
TLR2	1.5(0.75-2)	1.5(0.75-2.5)	1.5(0.75-2)	1.75(0.75-2.5)	0.416
TLR4	1.0(0.5-2)	1.25(0.5-2)	1.25(0.75-2.25)*	1.75(0.75-3)*	**0.008**
TLR9	0.5(0.12-0.75)	0.37(0.12-1)	0.5(0-1)	0.5(0.12-1.5)	0.851
CD14	0.62(0.5-1)	0.75(0.25-1.5)	0.75(0.5-1.75)	1.0(0.5-1.75)	0.338
NOD1	2.0(0.25-2.75)	2.5(1-3)	2.5(1-2.75)	2.5(2-3)*§	**0.022**
NOD2	0(0-0)	0(0-0)	0(0-0)	0(0-0.25)	0.784
MYD88	1.62(0.75-2.75)	1.62(0.75-2.5)	1.5(0.75-2)	2(0.75-2.5)	0.059
TIRAP	1.5(0.75-2.75)	2(1-2.5)	1.75(0.5-2.5)	2.37(1-2.75)	0.082
Phospho-IRAK1	1.5(0.75-2)	1.75(0.75-2.5)	1.5(1-2.5)	2(1-2.25)	0.688
IRAK4	2.5(1.5-3)	2.37(1-3)	2.62(1.75-3)	2.5(1.5-3)	0.326
Lamina Propria (cells/mm^2)					
TLR2	101(56-168)	124(45-185)	90(11-390)	150(12-470)	0.341
TLR4	62(46-129)	58(32-111)	99(40-285)&	111(27-344)&	**0.041**
TLR9	4(0-52)	5(0-15)	13(0-53)	4(0-90)	0.211
CD14	118(75-213)	133(21-376)	103(48-290)	161(60-312)	0.999
NOD1	153(37-355)	202(98-323)	229(145-419)*	286(161-475)*&	**0.007**
NOD2	0(0-9)	0(0-9)	0(0-11)	0(0-41)	0.780
MYD88	129(32-216)	128(44-275)	140(56-252)	138(44-339)	0.956
TIRAP	209(73-314)	176(101-376)	193(54-548)	258(39-548)	0.438
Phospho-IRAK1	322(232-441)	324(258-366)	344(185-419)	302(186-460)	0.550
IRAK4	155(70-406)	142(27-254)	206(64-387)	172(103-274)	0.071
CD4	164(101-212)	246(37-500)	258(107-731)	252(66-470)	0.206
CD8	147(76-301)	179(86-657)	195(86-523)	244(111-355)	0.365
CD68	284(128-516)	275(97-904)	367(158-759)	340(204-1054)	0.671
Neutrophil Elastase	93(58-166)	97(45-308)	94(28-512)	151(47-470)*&	0.045

27

28

Abbreviations: COPD, chronic obstructive pulmonary disease. Data expressed as median (range); n.d. not determined. Statistics: The Kruskal-Wallis test was used for multiple comparisons followed by Mann-Whitney U test for comparison between groups: *$p < 0.05$, significantly different from control non smokers; [&]$p < 0.05$, significantly different from control smokers with normal lung function; [§]$p < 0.05$, significantly different from mild/moderate COPD. The exact "p" values for comparison between groups are given in the Results section.

29

Table 3. Bacterial load in bronchial biopsies of COPD patients and control subjects

Bacterial load/mm²	Control non-smokers (n=5)	Control Smokers (n=9)	Mild/moderate COPD (n=13)	Severe/very severe COPD (n=15)	Kruskal Wallis (p value)
16S	5809±11269	4014±7126	6026±15477	810±1377	0.288
Pseudomonas aeruginosa	167±157 (78.8±23.3)	117±122 (67.2±22.6)	143±149 (77.2±23.9)	61±62 (88.8±20.2)	0.451 (0.050)
Haemophilus influenzae	42±59 (20.6±23.9)	51±74 (31.8±22.1)	28±38 (22.6±24.0)	5±8[&§] (10.7±20.5)[&§]	0.007 (0.029)
Moraxella catarrhalis	0.8±1.1 (0.6±1.3)	1±2.2 (0.7±1.9)	0.1±0.3 (0.07±0.26)	0.2±0.7 (0.47±1.25)	0.567 (0.924)
Streptococcus pneumoniae	0.06±0.13 (0.0±0.0)	0.0±0.0 (0.0±0.0)	0.11±0.34 (0.07±0.26)	0.0±0.0 (0.0±0.0)	0.710 (0.986)

Abbreviations: 16S=total bacterial load. The bacterial load (copies/ml) is normalized for bronchial biopsy superficial layer (mm²). In brackets is the percentage of each bacterium studied over the total load value including *P. aeruginosa+ H. influenza+ M. catarrhalis+ S. pneumonia*. Data expressed as mean±Standard Error. Statistics: The Kruskal-Wallis test was used for multiple comparisons followed by Mann-Whitney U test for comparison between groups: *p<0.05, significantly different from control non-smokers; [&]p<0.05, significantly different from control smokers with normal lung function; [§]p<0.05, significantly different from mild/moderate COPD. The exact "p" values for comparison between groups are given in the Results section.
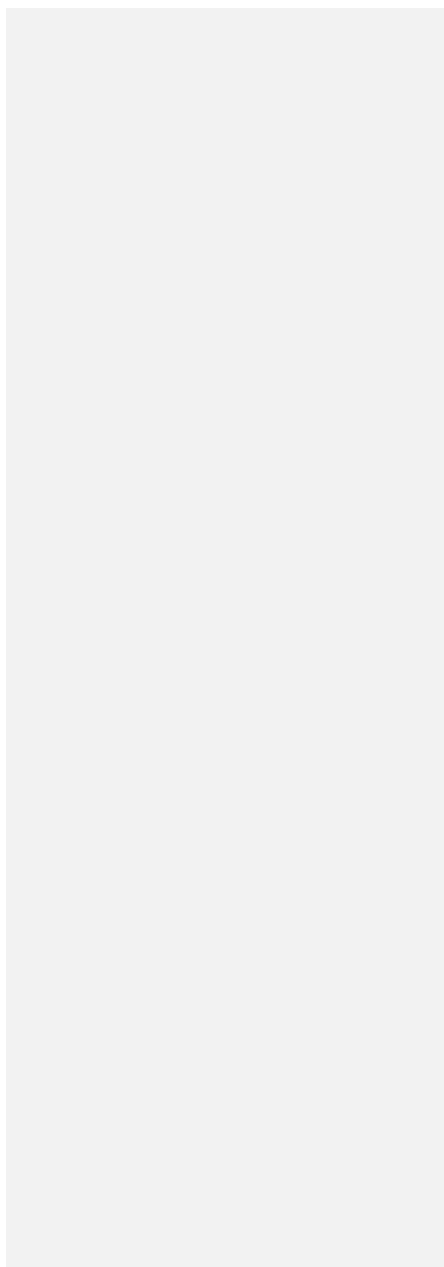
29

1
2
3
4
5
6
7
8
9
10
11
12
13
14
15
16
17
18
19
20
21
22
23
24
25
26
27
28
29
30
31
32
33
34
35
36
37
38
39
40
41
42
43
44
45
46
47
48
49
50
51
52
53
54
55
56
57
58
59
60

30

Figure Legends

Figure 1. Schematic representation of the molecular variations related to bacterial-related (panels a, b) molecules in the bronchial epithelium (panel a) and in the bronchial lamina propria (panel b) of control non-smokers, control smokers, mild/moderate stable COPD and severe/very severe stable COPD patients. With worsening of the disease, levels of TLR4 and NOD1 increase in bronchial epithelium (panel a) and in lamina propria (panel b). Panel (c) shows the *P. aeruginosa* and the *H. influenzae* variations in control subjects and in COPD patients of increasing severity. With worsening of the disease, levels of *P. aeruginosa* increase, while levels of *H. influenzae* decrease in bronchial biopsies. Panel (d) shows the TLR4 mRNA significant increase induced by H_2O_2 stimulation of bronchial epithelial cells (16HBE) at 2h after the oxidative stimulus. Data in panels a, b, c, d are expressed as median±Standard Error.

*significantly different from control non-smokers; &significantly different from control smokers; §significantly different from mild/moderate COPD. CNS=Control non-smokers; CS=Control smokers; M COPD=Mild/moderate COPD; S COPD=Severe/very severe COPD.

Figure 2. Regression analysis between TLR4 scored epithelial values and FEV1% predicted (panels a, c) and TLR4 scored epithelial values vs FEV1/FVC% (panels b, d). Correlations were performed in all smokers (panels a, b) and in patients with COPD alone (panels c, d). The lung functional indices of bronchial obstruction were significantly and inversely correlated to the immune expression of TLR4 in the bronchial epithelium of all smokers and of patients with COPD alone. Correlation coefficients were calculated using the Spearman rank method.

Figure 3. Regression analysis between FEV1% lung functional values and percentage of *P. aeruginosa* (panels a, c) and percentage of *H. influenzae* (panels b, d) in all smokers (panels a, b) and COPD patients (panels c, d). In the bronchial mucosa increased values of bronchial obstruction were associated to an increased percentage of *P. aeruginosa* in all smokers and a decreased percentage of *H. influenzae* in all smokers and patients with COPD.in the bronchial mucosa. Correlation coefficients were calculated using the Spearman rank method.

30

31

Figure 4. *TLR4 and NOD1 signaling in COPD.* In the presence of concomitant oxidative stress stimuli, pathogen-associated molecular patterns (PAMPs) from micro-organisms and endogenous molecules termed danger-associated molecular patterns (DAMPs) stimulate TLR4 leading to the recruitment of the TLR signaling adaptors myeloid differentiation primary response protein 88 (MYD88) and the adapter molecule toll-interleukin 1 receptor (TIR) domain containing adaptor protein (TIRAP). The MYD88 dependent pathway recruits the IL-1R-associated kinases (IRAKs) family of proteins which leads to IκB phosphorylation resulting in the activation and nuclear translocation of NF-κB which can be responsible for the over-expression of numerous inflammatory genes. TLR4, MYD88, TIRAP and p65 (NF-κB) result increased in COPD patients. Bacterial PG-derived peptides γ-D-glutamyl-m-diaminopimelic acid (iE-DAP) and muramyldipeptide (MDP) are recognized by the cytosolic receptors termed nucleotide-binding oligomerization domain (NOD)1 and NOD2. NOD1 and NOD2 through CARD-CARD interactions may stimulate downstream IKK complex which in turn, phosphorylates the NF-kB inhibitor IκBα followed by the NF-κB activation and nuclear translocation. Gram-negative bacteria preferentially activate NOD1 which was found up-regulated in our present study in COPD patients.

31

1

Bronchial inflammation and bacterial load in stable COPD is associated with TLR4 overexpression

Antonino Di Stefano, PhD[1], Fabio LM Ricciardolo, MD, PhD[2], Gaetano Caramori MD, PhD[3], Ian M Adcock, PhD[4], Kian Fan Chung MD[4], Peter J Barnes MD[4], Paola Brun, PhD[5], Andrea Leonardi, MD[6], Filippo Andò MD[7], Davide Vallese, PhD[1], Isabella Gnemmi[1], Luisella Righi, MD[8], Francesco Cappello, MD[9,10], Bruno Balbi, MD[1]

[1]Divisione di Pneumologia e Laboratorio di Citoimmunopatologia dell'Apparato Cardio Respiratorio, Istituti Clinici Scientifici Maugeri SpA, Società Benefit, Veruno (NO), Italy, [2]Dipartimento di Scienze Cliniche e Biologiche, A.O.U., San Luigi, Orbassano, Università di Torino, Italy, [3]Centro Interdipartimentale per lo Studio delle Malattie Infiammatorie delle Vie Aeree e Patologie Fumo-correlate (CEMICEF; formerly named Centro di Ricerca su Asma e BPCO), Sezione di Medicina Interna e Cardiorespiratoria, Università di Ferrara, [4]Airways Disease Section, National Heart and Lung Institute, Imperial College London, UK, [5]Dipartimento di Medicina Molecolare, Università di Padova, Italy, [6]Department of Neuroscience, Ophthalmology Unit, University of Padua, Padua, Italy; [7]UOC di Malattie Respiratorie, Dipartimento di Scienze Biomediche, Odontoiatriche e delle Immagini Morfologiche e Funzionali, Università di Messina, Italy, [8]Dipartimento di Oncologia, SCDU, Anatomia Patologica, A.O.U., San Luigi, Orbassano, Università di Torino, Italy [9]Dipartimento di Biomedicina Sperimentale e Neuroscienze Cliniche, Sezione di Anatomia Umana, Università di Palermo, Italy, [10]Euro-Mediterranean Institute of Science and Technology (IEMEST), Palermo, Italy.

Short title: Inflammation, bacterial load and active anti-bacterial immune response involving TLR4 and NOD1 in stable COPD

Conflict of interest: No conflict of interest for all the authors included in the present study

Manuscript word count: 3040

1

2

Correspondence to:

Dr Antonino Di Stefano, PhD,

Istituti Clinici Scientifici Maugeri, IRCCS,

Divisione di Pneumologia e Laboratorio di Citoimmunopatologia

dell'Apparato Cardio Respiratorio

Via per Revislate, 13

28010 Veruno (NO), Italy

tel: +39 0322 884711

fax: +39 0322 884776

E-mail: antonino.distefano@icsmaugeri.it

1
2
3
4
5
6
7
8
9
10
11
12
13
14
15
16
17
18
19
20
21
22
23
24
25
26
27
28
29
30
31
32
33
34
35
36
37
38
39
40
41
42
43
44
45
46
47
48
49
50
51
52
53
54
55
56
57
58
59
60

2

Abstract

Background: Toll-like receptors (TLRs) and nod-like receptors (NLRs) are two major forms of innate immune sensors but their role in the immunopathology of stable COPD is incompletely studied.

Objectives: To investigate TLRs and NLRs signaling pathways in the bronchial mucosa in stable COPD

Methods: Using immunohistochemistry the expression of TLR2, -4, -9, NOD1, NOD2, CD14, MYD88, TIRAP, pIRAK1, IRAK4 were measured in the bronchial mucosa of subjects with stable COPD of different severity (n=34), control smokers (n=12) and non-smokers (n=12). The bronchial bacterial load of *P. aeruginosa*, *H. influenzae*, *M. catarrhalis*, *S. pneumonie* was measured by qRT-PCR.

Results: TLR4 and NOD1 expression were increased in the bronchial mucosa of patients with severe/very severe stable COPD compared to control subjects. TLR4 bronchial epithelial expression correlated positively with CD4+ and CD8+ cells and the airflow obstruction. NOD1 expression correlated with CD8+ cells. The bronchial load of *P. aeruginosa* was directly correlated but *H. influenzae* inversely correlated with the degree of airflow obstruction. Bacterial load did not correlate with inflammatory cells.

Conclusions: Bronchial epithelial overexpression of TLR4 and NOD1 in severe/very severe stable COPD, associated with increased bronchial inflammation and *P. aeruginosa* bacterial load, may play a role in the pathogenesis of COPD.

Word count: 200

4

Key words

COPD pathology, bacterial load, innate immune response, toll-like receptors and nod-like receptors

Abbreviations:

FEV_1=forced expiratory volume in one second,

FVC= forced vital capacity.

iE-DAP=γ-D-glutamyl-meso-diaminopimelic acid,

IRAK=IL-1 receptor-associated kinase,

LPS=lipopolysaccharide,

MYD88=myeloid differentiation primary response gene 88,

NOD=nucleotide-binding oligomerization domain,

PAMP=pathogen-associated molecular patterns,

PGN=peptidoglycan,

PRR=pattern-recognition receptors,

TIRAP=TIR domain-containing adaptor protein,

TLR=toll-like receptor,

4

5

Introduction

Inflammation plays a key role in the pathogenesis of chronic obstructive pulmonary disease (COPD) (1). A symbiotic relationship between the microbiota and the innate and adaptive immune host response has been postulated (2, 3). Immune host responses to microbiota challenges are balanced in such a way as to maintain the microbiota diversity required for induction of protective responses to pathogens (2, 3). The innate immune system recognizes microbial pathogens through pattern-recognition receptors (PRRs), which detect the pathogen-associated molecular patterns (PAMPs) and induce inflammatory host responses and activation of the adaptive immune responses (2, 3).

Toll-like receptors (TLRs) and nucleotide-binding oligomerization domain (NOD)-like receptors (NLRs) are two major PRRs, which provide responses against pathogenic invasion or tissue injury (4). TLR2 recognizes lipoteichoic acid from Gram positive bacteria and some non-typical lipopolysaccharides (LPS) of Gram negative bacteria (5); TLR4 recognizes LPS and some endogenous ligands (5) and TLR9 is involved in viral A/D- and bacterial B/K-type CpG DNA recognition (6). CD14 acts as a co-receptor (along with TLR4) for the detection of (LPS) but can bind LPS only in the presence of lipopolysaccharide-binding protein (LBP). Although LPS is considered its main ligand, CD14 also recognizes other PAMPs such as lipoteichoic acid (7).

NOD1 and NOD2 recognize intracellular bacteria through identification of peptidoglycan (PGN) components, such as a muramyl dipeptide (MDP) found in almost all bacteria, or via γ-D-glutamyl-meso-diaminopimelic acid (iE-DAP) found in Gram-negative bacteria (8). Both myeloid differentiation primary response gene 88 (MYD88)-dependent and -independent (involving the CD14) signaling pathways are activated downstream of TLR activation (9, 10). Upon receptor stimulation, MYD88 recruits interleukin-1 receptor-associated kinase (IRAK)-4 to TLRs and induces IRAK-1 phosphorylation, followed, in turn, by AP-1 activation and nuclear translocation and/or IκB degradation and NF-κB

5

nuclear activation (11-14). TIR domain-containing adaptor protein (TIRAP) is essential for

the MYD88-dependent signaling pathway through TLR2 and TLR4 activation (15).

Abnormalities in any of these innate sensor-mediated processes may result in excessive

inflammation due to either hyperactive innate immune signaling or sustained

compensatory adaptive immune activation (4, 5). These characteristics have been

observed in the lower airways of patients with stable COPD (1). We hypothesize the

detection of bacterial proteins occurs to a greater extent in more severe COPD. The aim

of this study was to investigate TLRs and NLRs signaling pathways in the bronchial

mucosa in relation to the bronchial bacterial load of patients with stable COPD of differing

severity and control subjects.

Methods

Subjects

All COPD patients and control subjects who underwent bronchoscopy and bronchial biopsies were recruited from the Respiratory Medicine Unit of the Fondazione Salvatore Maugeri, Institute of Veruno (Veruno, Italy). In COPD patients, the severity of the airflow obstruction was graded using current GOLD criteria [http://goldcopd.org/]. All former smokers had stopped smoking for at least one year. COPD and chronic bronchitis were defined, according to international guidelines, [http://goldcopd.org/]. All COPD patients were stable with no exacerbation in the six months prior to bronchoscopy. None of the subjects was treated with theophylline, antibiotics, antioxidants, mucolytics, and/or glucocorticoids in the month prior bronchoscopy. The study conformed to the Declaration of Helsinki and was approved by the ethics committees of the Fondazione Salvatore Maugeri [Veruno (Novara), Italy], the University Hospital of Ferrara, Italy. Written informed consent was obtained from each subject and bronchial biopsies were performed according to the local ethic committee guidelines.

A detailed description of subjects, lung function tests, fibreoptic bronchoscopy and processing of bronchial biopsies, immunohistochemistry, scoring system for immunohistochemistry, double staining, quantification of bacterial load and "*in vitro*" experiments performed on normal human bronchial epithelial (NHBE) cells and details of statistical analysis are provided in the supplementary material.

Statistical analysis

The numbers of patients used in each group was based on previous studies which examined differences in inflammatory cell numbers in bronchial biopsies (16). Differences between groups were analyzed using analysis of variance (ANOVA) for functional data. The ANOVA test was followed by the unpaired t-test for comparison between groups. The

8

Kruskal-Wallis test applied for morphologic data was followed by the Mann-Whitney U test for comparison between groups. Correlation coefficients were calculated using the Spearman rank method. Probability values of $p<0.05$ were considered significant.

Results

Clinical characteristics of the subjects

We obtained and studied bronchial biopsies from 58 subjects: 34 with stable COPD, 12 control smokers with normal lung function, and 12 non-smokers with normal lung function (**Table 1**). COPD patients were divided into two groups: mild/moderate (GOLD stage I-II, n=16) and severe/very severe GOLD stage III-IV, n=18) [www.goldcopd.org]. There was no difference in age between the subjects in the four groups. The smoking history was similar in the three smoking groups. Values of FEV_1 (% predicted) and FEV_1/FVC (%) differed significantly between total COPD patients (mild/moderate and severe/very severe) and both control groups (healthy smokers and healthy non-smokers). Lung function in severe/very severe COPD patients also differed significantly from mild/moderate COPD patients (ANOVA: $p < 0.0001$ for FEV_1% predicted and FEV_1/FVC% values). Thirty-five percent (n=12) of the total COPD patients and 25% (n=3) of healthy smokers with normal lung function also had symptoms of chronic bronchitis but this was not significant.

Inflammatory cells in the bronchial biopsies

The results of the immunohistochemical analysis are summarised in **Table 2**. These data, obtained from stable COPD patients, confirm previously reported results showing higher numbers of neutrophils in severe/very severe COPD (**Table 2**) (16). There was also a trend towards increased CD8+ cell numbers in severe and very severe patients but this did not reach significance according to the Kruskal-Wallis test. COPD patients with chronic bronchitis had a similar number of neutrophils when compared with COPD patients without chronic bronchitis (16, 17).

Immunohistochemistry

The results of the immunohistochemical study for the TLRs and NLRs signaling pathways

are summarized in **Table 2**.

Immunohistochemistry in bronchial epithelium

The expression of TLR4 in the bronchial epithelium was increased in severe/very severe stable COPD compared to non-smoking control subjects (p=0.0027) (**Table 2, Figure E1**). There was a trend towards significance between these COPD patients and control smokers with normal lung function (p=0.054). The expression of TLR4 in the bronchial epithelium was also increased in mild/moderate stable COPD patients compared with non-smoking control subjects (p=0.024). Similarly, the expression of NOD1 in the bronchial epithelium was increased in severe/very severe stable COPD compared to mild/moderate stable COPD patients (p=0.036) and non-smoking control subjects (p=0.006) (**Table 2, Figure E2**). NOD1 expression also trended towards significance between severe/very severe stable COPD patients and control smokers with normal lung function (p=0.054).

The bronchial epithelial expression of both MYD88 (Kruskal-Wallis:p=0.059, Mann-Whitney:p=0.012 and p=0.038, respectively) and TIRAP (Kruskal-Wallis:p=0.082, Mann-Whitney:p=0.035 and p=0.047, respectively) also tended to be increased in severe/very severe stable COPD patients compared to mild/moderate COPD and control smokers with normal lung function (**Table 2**). No significant differences were observed for the other molecules studied (**Table 2**). These data are also summarized in **Figure 1A**.

Immunohistochemistry in bronchial lamina propria

TLR4 was increased in severe/very severe COPD (p=0.027) and mild/moderate COPD (p=0.015) compared to control smokers (**Table 2, Figure E1**). NOD1 was increased in severe/very severe COPD compared to control smokers (p=0.022) and control non-smokers (p=0.002). It was also increased in mild/moderate COPD (p=0.023) compared to control non-smokers (**Table 2, Figure E2**). IRAK4 tended to be increased in mild/moderate

COPD (Kruskal-Wallis: p=0.071, Mann Whitney: p=0.017) compared to control smokers (**Table 2**). No statistical differences were observed for the other molecules studied (**Table 2**). These data are summarized in **Figure 1B**. Double staining for identification of CD8+ (T-cell), CD68+ (macrophage) and CD31+ (endothelial) cells co-expressing TLR4 and NOD1 was performed in three representative COPD patients. The percentage of (mean±s.e.) CD8+ TLR4+, CD68+TLR4+ and CD31+TLR4+ double stained cells were 51±11%, 54±12% and 61±5%, respectively; the percentage of CD8+ NOD1+, CD68+NOD1+ and CD31+NOD1+ double stained cells were 31±10%, 30±5% and 43±5%, respectively (**Figure E3**).

Quantification of bacterial load in the bronchial biopsies

The results of the quantification of the bacterial load in bronchial biopsies are summarized in **Table 3** and **Figure 1C**. When data were expressed as absolute numbers, *H. influenzae* was decreased in severe/very severe COPD compared to mild/moderate COPD (p=0.011) and control smokers (p=0.0013). No significant differences were observed for *P. aeruginosa*, *M. catarrhalis* and *S. pneumoniae* (**Table 3**). To evaluate changes on the relative proportions of each bacterium studied, we expressed these data as percentage of the total load value constituted by the sum of the four bacteria studied. The percentage of *P. aeruginosa* tended to be increased in severe/very severe stable COPD compared to control smokers with normal lung function (Kruskal Wallis: p=0.050, Mann-Whitney: p=0.012); the percentage of H. *influenzae* was significantly decreased in severe/very severe COPD compared to mild/moderate COPD (p=0.029) and control smokers (p=0.010) (**Table 3, Figure 1C**).

Quantification of TLR4 mRNA in "in vitro" H_2O_2 treated bronchial epithelial cells.

12

Bronchial epithelial (16HBE) cells treated with H_2O_2 (100μM) showed significantly increased TLR4 mRNA levels after 2h (**Figure 1D**).

Correlations between clinical parameters, number of inflammatory cells, TLRs and NLRs signaling pathways expression and bacterial load in the bronchial biopsies

In all smokers, the degree of TLR4 immunostaining in the bronchial epithelium was positively correlated with the numbers of CD8+ cells (r=0.630, p=0.018) and CD4+ cells (r=0.580, p=0.029) in the bronchial lamina propria. In addition, in all smokers, the degree of TLR4 immunostaining in bronchial epithelium was inversely correlated with the FEV_1% of the predicted (r=-0.36, p=0.019) and the FEV_1/FVC% (r=-0.39, p=0.009). When the analysis was restricted to patients with stable COPD alone, the correlations between the degree of TLR4 immunostaining in the bronchial epithelium with FEV1% predicted (r=-0.37, p=0.037) and FEV_1/FVC ratio (r=-0.50, p=0.005) was maintained (**Figure 2**). In all smokers, NOD1 immunostaining in the lamina propria was inversely correlated with the FEV_1% predicted values (r=-0.39, p=0.019) and positively correlated with the numbers of CD8+ cells (r= 0.538, p=0.044).

Interestingly, in all smokers, the bronchial load of *P. aeruginosa* was inversely correlated with the FEV_1% of the predicted values (r=-0.41, p=0.012) (**Figure 3**); whereas the reverse effect was seen with the bronchial load of *H. influenzae* which was positively correlated with the FEV_1% of the predicted (r=0.458, p=0.005) (**Figure 3**). This association was maintained in the COPD patient group when studied separately (r=0.424, p=0.025).

No other statistically significant correlations were found between clinical parameters, expression of bacterial receptors, number of inflammatory cells and bacterial load.

Discussion

We have shown here that TLR4 and NOD1 protein expression is enhanced in the bronchial mucosa of patients with severe/very severe COPD compared to control subjects. In addition the bronchial epithelial expression of TLR4 correlates positively with the numbers of CD4+ and CD8+ cells in the bronchial mucosa and with the degree of airflow obstruction. NOD1 expression also correlated with CD8+ cell numbers. The degree of airflow obstruction was positively correlated with an increased load of *P. aeruginosa* and a decreased load of *H. influenzae* in the bronchial biopsies in all smokers and in patients with stable COPD.

A previous study found no significant differences in TLR4 expression in the bronchial mucosa of mild/moderate stable COPD patients compared to control subjects, while the percentage of CD8+ cells co-expressing TLR4 was increased (18). The difference between the results reported here could be due to the low number of COPD (n=8) and control subjects (n=5) studied (18) and also due to the different severity of the COPD patients. In all smokers and patients with COPD, we found a significant positive correlation between TLR4 epithelial expression and numbers of CD8+ and CD4+ cells in the lamina propria, showing an association between bronchial inflammation and upregulation of TLR4 in stable COPD. Furthermore, in agreement with our present data, increased TLR4 expression was reported by Western blotting in GOLD stage 4 COPD patients compared to control non-smokers (19). In contrast, Lee and colleagues reported decreased TLR4 levels associated with increased bronchial obstruction and increased emphysema score on lung lysates of smokers (20) confirming the need for further investigations to correctly position our present data. We here showed that CD8+, CD68+ and CD31+ cells mainly contributed to the up-regulation of TLR4 and NOD1 in bronchial biopsies of COPD patients. In agreement, using flow cytometric analysis, CD8+ cells co-

14

expressing TLR4 were also increased in the peripheral lung tissue of COPD patients compared to control smokers (21).

TLR4 recognises lipopolysaccharides (LPS), the major surface component of Gram-negative bacteria (5). Lipid A is the pro-inflammatory component of LPS and TLR4 is required for the recognition of lipid A of *P. aeruginosa* (22) suggesting that its overexpression in the bronchial epithelium of severe/very severe stable COPD patients may be important for sensing and responding to persistent colonization of the lower airways of these patients (23). Interestingly, *in vitro,* TLR4 activates NF-κB and propagate and maintain oxidative/nitrosative cellular stress that are both involved in the pathogenesis of stable COPD (1, 24).

Oxidative stress is more pronounced in advanced COPD (1) and *in vitro* both tobacco smoking exposure (18) and oxidative stress (25) may upregulate TLR4 expression. In our *in vitro* experiments, using human bronchial epithelial cells (16HBE) treated with H_2O_2, we showed that oxidative stress induced TLR4 mRNA. Recent evidence in smoking mice (26) indicates that cigarette smoke significantly enhanced *tlr4* mRNA expression after 4 (1.77 fold) and 12 weeks (1.53 fold). Furthermore, ozone enhanced *tlr4* mRNA in the lungs of mice after 6 weeks of exposure is completely ablated by treatment with N-acetylcysteine (unpublished data). This data, taken together, indicates that increased oxidative stress could be capable of up-regulating TLR4 also in the bronchi of stable COPD patients, although specific studies in humans need to be performed to confirm this hypothesis.

We also demonstrated increased expression of NOD1 in bronchial epithelium and lamina propria of stable COPD patients compared to control subjects, suggesting an involvement of this cytosolic protein in the recognition process of bacterial cell wall components in the bronchial mucosa of patients with stable COPD (27). *In vitro* human bronchial epithelial cells challenged with *M. catarrhalis* show an increased CXCL-8

14

expression that is blocked by NOD1 inhibitors (28). In addition, *in vitro* NOD1 agonists activates NF-κB in human endothelial cells (29), supporting the role of NOD1 in sustaining bronchial inflammation.

The increased expression of MYD88 in the bronchial epithelium of patients with severe/very severe stable COPD compared to control smokers with normal lung function, without significant differences in CD14 expression, suggests the involvement of a MYD88-dependent downstream signaling pathway in the immunopathology of the bronchial mucosa of stable COPD patients. This is in keeping with our data showing increased expression of TIRAP in the bronchial epithelium of our severe/very severe COPD patients, an index of MYD88-dependent pathway activation (15) **(Figures 1 and 4)**.

The decreased *H. influenzae* load observed in the bronchial mucosa of our patients with severe/very severe stable COPD compared to mild/moderate COPD and control smokers with normal lung function is in keeping with previous studies showing a fundamental role of TLR4 activation in the clearance of this bacteria from the mouse lung (30, 31). This is also in agreement with previous studies showing that *H. influenzae* is virtually absent in severe/very severe COPD lung tissues and increased in milder forms of COPD (32). The absence of *H. influenzae* may also provide a niche for colonization by other pathogenic bacteria such as new strains of *P. aeurginosa* (32, 33).

Our data on the bronchial bacterial load are discordant with a previous study performed in lung parenchymal tissues. This showed no significant differences in total bacterial load between advanced stable COPD and control subjects (34) and may reflect the different lower airway compartment examined. Previous studies have clearly demonstrated a progressive decrease of the total bacterial load from upper to lower airways and lung parenchyma (32, 33, 35), and this makes more difficult to identify significant differences between patients with stable COPD of different severities and control subjects in the presence of very low levels of total bacterial load. This difference

16

may also influence the related immune host response developing in the bronchi and lung tissue (different compartments) of COPD patients when compared to control subjects. These considerations are also reinforced by the data of Cabrera-Rubio et al. (36) showing that in patients with stable COPD the microbiota composition obtained by the analysis of bronchial biopsies and bronchoalveolar lavage better represents the lower airway bacterial composition compared to the analysis of sputum and bronchial aspirate samples (36).

Neither *P. aeruginosa* nor *H. influenzae,* expressed as absolute number or as percentage, were correlated with inflammatory cells (CD8+, CD68+ neutrophils) or bacterial-related molecules (TLR4, NOD1) mainly expressed in the bronchial biopsies. This finding suggests that in stable disease the microbiota may not be directly related to the classical COPD inflammatory response developing in the bronchial mucosa. This seems to be in contrast to the situation during COPD exacerbations where a concomitant increase of bronchial inflammation (37), microbiota load (38) and TLR4 expression (39) has been observed. However, a comprehensive study of pathogen-related bacteria and related inflammatory response in bronchial biopsies of exacerbated COPD patients is lacking. Furthermore, changes in microbial composition in the lung and gut have been linked to organ-related alterations of the immune responses. However, no studies have investigated changes in the gut microbiota of patients with COPD of increasing severity (40).

It is interesting to note that certain single nucleotide polymorphisms (SNPs) of the NOD2 gene were associated with more severe disease in Japanese COPD patients (41) and this area deserves more research in the future. Furthermore, our current study, the expression of both IRAK4 and pIRAK1, which favor NF-κB nuclear activation (11), were both over expressed in the bronchial epithelium and lamina propria of all subjects studied. This indicates that the bronchial mucosa is activated in COPD (**Figures 1 and 4**). A more

16

expansive study using next generation sequencing may determine the precise differences in inflammation and immunity in these patients.

As a limitation of this study, and in agreement with other authors (33), we cannot exclude a bias in the quantification of the bacterial load due to repeated antibiotic treatments, particularly in severe/very severe COPD patients, even though a one-month wash-out period from antibiotic treatments was applied in our protocol study.   In addition, the study was not powered to detect the effect of smoking cessation on these parameters and further larger studies are required to confirm these data as well as the subgroup analysis performed here.

In conclusion, the overexpression of TLR4 and NOD1 in the bronchial epithelium of patients with severe/very severe stable COPD, associated to increased bronchial inflammation and *P. aeruginosa* bacterial load may play a role in the pathogenesis of the disease.

18

Acknowledgements

Author contributions: ADS, FLMR, GC, DV, FC contributed to the study design, interpretation of the data and in writing the manuscript; AC, IAB, PJB, KFC, FA, PB, AL, LR, BB contributed to a critical revision of the manuscript; IG, VS, DV, ADS contributed to the production of the data and accuracy of the data analysis.

19

References

1. **Barnes PJ.** Cellular and molecular mechanisms of chronic obstructive pulmonary disease. Clin Chest Med. 2014;35:71-86.

2. **Belkaid Y, Hand TW.** Role of the microbiota in immunity and inflammation. Cell. 2014;157:121-141.

3. **Iwasaki A, Medzhitov R.** Control of adaptive immunity by the innate immune system. Nat Immunol. 2015;16:343-353.

4. **Fukata M, Vamadevan AS, Abreu MT.** Toll-like receptors (TLRs) and Nod-like receptors (NLRs) in inflammatory disorders. Semin Immunol. 2009;21:242-53.

5. **Takeda K, Akira S.** Toll-like receptors in innate immunity. Int Immunol. 2005;17:1-14.

6. **Lund J, Sato A, Akira S, Medzhitov R, Iwasaki A.** Toll-like receptor 9-mediated recognition of Herpes simplex virus-2 by plasmacytoid dendritic cells. J Exp Med. 2003;198:513-520.

7. **Ranoa DR, Kelley SL, Tapping RI.** Human lipopolysaccharide-binding protein (LBP) and CD14 independently deliver triacylated lipoproteins to Toll-like receptor 1 (TLR1) and TLR2 and enhance formation of the ternary signaling complex. J Biol Chem. 2013;288:9729-41.

8. **Girardin SE, Boneca IG, Viala J, Chamaillard M, Labigne A, Thomas G, Philpott DJ, Sansonetti PJ.** Nod2 is a general sensor of peptidoglycan through muramyl dipeptide (MDP) detection. J Biol Chem. 2003;278:8869-8872.

9. **Hemmi H**, **Kaisho T**, **Takeda K**, **Akira S**. The roles of Toll-like receptor 9, MyD88, and DNA-dependent protein kinase catalytic subunit in the effects of two distinct CpG DNAs on dendritic cell subsets. J Immunol. 2003;170:3059-3064.

10. **Ito T, Amakawa R, Kaisho T, Hemmi H, Tajima K, Uehira K, Ozaki Y, Tomizawa H, Akira S, Fukuhara S**. Interferon-alpha and interleukin-12 are induced differentially by Toll-

20

like receptor 7 ligands in human blood dendritic cell subsets. J Exp Med. 2002;195:1507-1512.

11. **Takeuchi O**, **Takeda K**, **Hoshino K, Adachi O, Ogawa T, Akira S.** Cellular responses to bacterial cell wall components are mediated through MyD88-dependent signaling cascades. Int Immunol. 2000;12:113-117.

12. **Kawai T, Adachi O, Ogawa T, Takeda K, Akira S.** Unresponsiveness of MyD88-deficient mice to endotoxin. Immunity. 1999;11:115-122.

13. **Schnare M, Holt AC, Takeda K, Akira S, Medzhitov R.** Recognition of CpG DNA is mediated by signaling pathways dependent on the adaptor protein MyD88. Curr Biol. 2000;10:1139-1142.

14. **Häcker H, Vabulas RM, Takeuchi O, Hoshino K, Akira S, Wagner H.** Immune cell activation by bacterial CpG-DNA through myeloid differentiation marker 88 and tumor necrosis factor receptor-associated factor (TRAF)6. J Exp Med. 2000;192:595-600.

15. **Yamamoto M**, **Sato S**, **Hemmi H**, **Sanjo H, Uematsu S, Kaisho T, Hoshino K, Takeuchi O, Kobayashi M, Fujita T, Takeda K, Akira S.** Essential role for TIRAP in activation of the signalling cascade shared by TLR2 and TLR4. Nature. 2002;420:324-329.

16**. Di Stefano A, Caramori G, Barczyk A, Vicari C, Brun P, Zanini A, Cappello F, Garofano E, Padovani A, Contoli M, Casolari P, Durham AL, Chung KF, Barnes PJ, Papi A, Adcock I, Balbi B.** Innate immunity but not NLRP3 inflammasome activation correlates with severity of stable COPD. Thorax. 2014;69:516-524.

17. **Vallese D, Ricciardolo FL, Gnemmi I, Casolari P, Brun P, Sorbello V, Capelli A, Cappello F, Cavallesco GN, Papi A, Chung KF, Balbi B, Adcock IM, Caramori G, Di Stefano A.** Phospho-p38 MAPK expression in COPD patients and asthmatics and in challenged bronchial epithelium. Respiration. 2015;89:329-342.

18**. Nadigel J, Préfontaine D, Baglole CJ, Maltais F, Bourbeau J, Eidelman DH, Hamid Q.** Cigarette smoke increases TLR4 and TLR9 expression and induces cytokine

production from CD8(+) T cells in chronic obstructive pulmonary disease. Respir Res. 2011;12:149. doi: 10.1186/1465-9921-12-149.

19. **An CH, Wang XM, Lam HC, Ifedigbo E, Washko GR, Ryter SW, Choi AM.** TLR4 deficiency promotes autophagy during cigarette smoke-induced pulmonary emphysema. Am J Physiol Lung Cell Mol Physiol. 2012 Nov 1;303(9):L748-57.

20. **Lee SW, Kim DR, Kim TJ, Paik JH, Chung JH, Jheon S, Huh JW, Lee JH, Lee CT.** The association of down-regulated toll-like receptor 4 expression with airflow limitation and emphysema in smokers. Respir Res. 2012 Nov 21;13:106.

21. **Freeman CM, Martinez FJ, Han MK, Washko GR Jr, McCubbrey AL, Chensue SW, Arenberg DA, Meldrum CA, McCloskey L, Curtis JL**. Lung CD8+ T cells in COPD have increased expression of bacterial TLRs. Respir Res. 2013 Feb 1;14:13.

22. **Ernst RK, Hajjar AM, Tsai JH, Moskowitz SM, Wilson CB, Miller SI.** Pseudomonas aeruginosa lipid A diversity and its recognition by Toll-like receptor 4. J Endotoxin Res. 2003;9:395-400.

23. **Gallego M, Pomares X, Espasa M, Castañer E, Solé M, Suárez D, Monsó E, Montón C.** Pseudomonas aeruginosa isolates in severe chronic obstructive pulmonary disease: characterization and risk factors. BMC Pulm Med. 2014;14:103. doi: 10.1186/1471-2466-14-103.

24. **Karki R**, **Igwe OJ.** Toll-like receptor 4-mediated nuclear factor kappa B activation is essential for sensing exogenous oxidants to propagate and maintain oxidative/nitrosative cellular stress. PLoS One. 2013;8:e73840. doi: 10.1371/journal.pone.0073840. eCollection 2013.

25. **Lucas K, Maes M.** Role of the Toll Like receptor (TLR) radical cycle in chronic inflammation: possible treatments targeting the TLR4 pathway. Mol Neurobiol. 2013;48:190-204. doi: 10.1007/s12035-013-8425-7.

26. **Haw TJ, Starkey MR Pavlidis S, Nair PM, Liu G, Hanish I,. Kim RY, Foster PS, Adcock IM, Horvat JC, Hansbro PM.** TLR2 and TLR4 have Opposing Roles in the Pathogenesis of Cigarette Smoke-induced COPD Am J Respir Cell Mol Biol 2016 (in press).

27. **Leissinger M, Kulkarni R, Zemans RL, Downey GP, Jeyaseelan S**. Investigating the role of nucleotide-binding oligomerization domain-like receptors in bacterial lung infection. Am J Respir Crit Care Med. 2014;189:1461-1468.

28. **Slevogt H**, **Seybold J**, **Tiwari KN, Hocke AC, Jonatat C, Dietel S, Hippenstiel S, Singer BB, Bachmann S, Suttorp N, Opitz B.** Moraxella catarrhalis is internalized in respiratory epithelial cells by a trigger-like mechanism and initiates a TLR2- and partly NOD1-dependent inflammatory immune response. Cell Microbiol. 2007;9:694-707.

29. **Gatheral T, Reed DM, Moreno L, Gough PJ, Votta BJ, Sehon CA, Rickard DJ, Bertin J, Lim E, Nicholson AG, Mitchell JA.** A key role for the endothelium in NOD1 mediated vascular inflammation: comparison to TLR4 responses. PLoS One. 2012;7:e42386.

30. **Wang X, Moser C, Louboutin JP, Lysenko ES, Weiner DJ, Weiser JN, Wilson JM.** Toll-like receptor 4 mediates innate immune responses to Haemophilus influenzae infection in mouse lung. J Immunol. 2002;168:810-815.

31. **Wieland CW, Florquin S, Maris NA, Hoebe K, Beutler B, Takeda K, Akira S, van der Poll T**. The MyD88-dependent, but not the MyD88-independent, pathway of TLR4 signaling is important in clearing nontypeable haemophilus influenzae from the mouse lung. J Immunol. 2005;175:6042-6049.

32. **Sze MA, Dimitriu PA, Suzuki M, McDonough JE, Campbell JD, Brothers JF, Erb-Downward JR, Huffnagle GB, Hayashi S, Elliott WM, Cooper J, Sin DD, Lenburg ME,**

Spira A, Mohn WW, Hogg JC. Host Response to the Lung Microbiome in Chronic Obstructive Pulmonary Disease. Am J Respir Crit Care Med. 2015;192:438-445.

33. **Dickson RP, Erb-Downward JR, Huffnagle GB.** Homeostasis and its disruption in the lung microbiome. Am J Physiol Lung Cell Mol Physiol. 2015;309:L1047-1055.

34. **Sze MA, Dimitriu PA, Hayashi S, Elliott WM, McDonough JE, Gosselink JV, Cooper J, Sin DD, Mohn WW, Hogg JC.** The lung tissue microbiome in chronic obstructive pulmonary disease. Am J Respir Crit Care Med. 2012;185:1073-1080.

35. **Charlson ES, Bittinger K, Haas AR, Fitzgerald AS, Frank I, Yadav A, Bushman FD, Collman RG.** Topographical continuity of bacterial populations in the healthy human respiratory tract. Am J Respir Crit Care Med. 2011;184:957-963.

36. **Cabrera-Rubio R, Garcia-Núñez M, Setó L, Antó JM, Moya A, Monsó E, Mira A.** Microbiome diversity in the bronchial tracts of patients with chronic obstructive pulmonary disease J Clin Microbiol. 2012;50:3562-3568.

37. **Saetta M, Di Stefano A, Maestrelli P, Turato G, Ruggieri MP, Roggeri A, Calcagni P, Mapp CE, Ciaccia A, Fabbri LM.** Airway eosinophilia in chronic bronchitis during exacerbations. Am J Respir Crit Care Med. 1994;150:1646-52.

38. **D'Anna SE, Balbi B, Cappello F, Carone M, Di Stefano A.** Bacterial-viral load and the immune response in stable and exacerbated COPD: significance and therapeutic prospects. Int J Chron Obstruct Pulmon Dis. 2016;11:445-453.

39. **Pace E, Ferraro M, Giarratano A, Cipollina C, Gjomarkaj M.** TLR4 up-regulation and reduced Foxp3 expression in mechanically ventilated smokers with obstructive chronic bronchitis. COPD. 2013 Apr;10(2):147-55.

40. **Budden KF, Gellatly SL, Wood DL, Cooper MA, Morrison M, Hugenholtz P, Hansbro PM.** Emerging pathogenic links between microbiota and the gut-lung axis. Nat Rev Microbiol. 2017; 15(1):55-63. doi: 10.1038/nrmicro.2016.142. Epub 2016 Oct 3.

24

41. **Kinose D, Ogawa E, Hirota T, Ito I, Kudo M, Haruna A, Marumo S, Hoshino Y, Muro S, Hirai T, Sakai H, Date H, Tamari M, Mishima M**. A NOD2 gene polymorphism is associated with the prevalence and severity of chronic obstructive pulmonary disease in a Japanese population. Respirology. 2012;17:164-171.

1
2
3
4
5
6
7
8
9
10
11
12
13
14
15
16
17
18
19
20
21
22
23
24
25
26
27
28
29
30
31
32
33
34
35
36
37
38
39
40
41
42
43
44
45
46
47
48
49
50
51
52
53
54
55
56
57
58
59
60

24

25

Tables

Table 1. Clinical characteristics of COPD and control subjects who provided bronchial biopsies

Groups	n	Age (years)	M/F	Pack years	Ex/current smokers	FEV$_1$ (%pred) pre-β_2	FEV$_1$ (%pred) Post-β_2	FEV$_1$/FVC (%)
Control non-smokers	12	63±13	10/2	0	0	117±18	ND	86±10
Control smokers with normal lung function	12	61±7	9/3	43±26	2/10	104±13	ND	81±6
COPD stages I and II (mild/moderate)	16	71±8	14/3	50±28	6/11	63±11[#]	67±13	57±9[#]
COPD stages III and IV (severe/very severe)	18	66±9	11/7	54±36	13/5	35±8[#&]	38±9	44±10[#&]

Patients were classified according to GOLD (http://goldcopd.org) levels of severity for COPD into: mild (stage I), moderate (stage II), severe (stage III), and very severe (stage IV). Data are mean±SD. For COPD patients FEV$_1$/FVC (%) are post-bronchodilator values. Abbreviations: M, male; F, female, FEV$_1$: forced expiratory volume in one second; FVC, forced vital capacity; ND, not determined; COPD, chronic obstructive pulmonary disease. Statistics. (ANOVA) [#]$p<0.0001$, significantly different from control smokers with normal lung function and control never-smokers; [&]$p<0.0001$, significantly different from mild/moderate COPD: (ANOVA)

25

26

Table 2. Immunohistochemical quantification of innate immune molecules and cytokines related to bacterial response in bronchial biopsies

	Control non Smokers	Control Smokers	Mild/Moderate COPD	Severe/very Severe COPD	Kruskal Wallis p value
Epithelium (score 0-3)					
TLR2	1.5(0.75-2)	1.5(0.75-2.5)	1.5(0.75-2)	1.75(0.75-2.5)	0.416
TLR4	1.0(0.5-2)	1.25(0.5-2)	1.25(0.75-2.25)*	1.75(0.75-3)*	**0.008**
TLR9	0.5(0.12-0.75)	0.37(0.12-1)	0.5(0-1)	0.5(0.12-1.5)	0.851
CD14	0.62(0.5-1)	0.75(0.25-1.5)	0.75(0.5-1.75)	1.0(0.5-1.75)	0.338
NOD1	2.0(0.25-2.75)	2.5(1-3)	2.5(1-2.75)	2.5(2-3)*§	**0.022**
NOD2	0(0-0)	0(0-0)	0(0-0)	0(0-0.25)	0.784
MYD88	1.62(0.75-2.75)	1.62(0.75-2.5)	1.5(0.75-2)	2(0.75-2.5)	0.059
TIRAP	1.5(0.75-2.75)	2(1-2.5)	1.75(0.5-2.5)	2.37(1-2.75)	0.082
Phospho-IRAK1	1.5(0.75-2)	1.75(0.75-2.5)	1.5(1-2.5)	2(1-2.25)	0.688
IRAK4	2.5(1.5-3)	2.37(1-3)	2.62(1.75-3)	2.5(1.5-3)	0.326
Lamina Propria (cells/mm^2)					
TLR2	101(56-168)	124(45-185)	90(11-390)	150(12-470)	0.341
TLR4	62(46-129)	58(32-111)	99(40-285)&	111(27-344)&	**0.041**
TLR9	4(0-52)	5(0-15)	13(0-53)	4(0-90)	0.211
CD14	118(75-213)	133(21-376)	103(48-290)	161(60-312)	0.999
NOD1	153(37-355)	202(98-323)	229(145-419)*	286(161-475)*&	**0.007**
NOD2	0(0-9)	0(0-9)	0(0-11)	0(0-41)	0.780
MYD88	129(32-216)	128(44-275)	140(56-252)	138(44-339)	0.956
TIRAP	209(73-314)	176(101-376)	193(54-548)	258(39-548)	0.438
Phospho-IRAK1	322(232-441)	324(258-366)	344(185-419)	302(186-460)	0.550
IRAK4	155(70-406)	142(27-254)	206(64-387)	172(103-274)	0.071
CD4	164(101-212)	246(37-500)	258(107-731)	252(66-470)	0.206
CD8	147(76-301)	179(86-657)	195(86-523)	244(111-355)	0.365
CD68	284(128-516)	275(97-904)	367(158-759)	340(204-1054)	0.671
Neutrophil Elastase	93(58-166)	97(45-308)	94(28-512)	151(47-470)*&	0.045

26

27

Abbreviations: COPD, chronic obstructive pulmonary disease. Data expressed as median (range); n.d. not determined. Statistics: The Kruskal-Wallis test was used for multiple comparisons followed by Mann-Whitney U test for comparison between groups: *$p<0.05$, significantly different from control non smokers; [&]$p<0.05$, significantly different from control smokers with normal lung function; [§]$p<0.05$, significantly different from mild/moderate COPD. The exact "p" values for comparison between groups are given in the Results section.

28

Table 3. Bacterial load in bronchial biopsies of COPD patients and control subjects

Bacterial load/mm^2	Control non-smokers (n=5)	Control Smokers (n=9)	Mild/moderate COPD (n=13)	Severe/very severe COPD (n=15)	Kruskal Wallis (p value)
16S	5809±11269	4014±7126	6026±15477	810±1377	0.288
Pseudomonas aeruginosa	167±157 (78.8±23.3)	117±122 (67.2±22.6)	143±149 (77.2±23.9)	61±62 (88.8±20.2)	0.451 (0.050)
Haemophilus influenzae	42±59 (20.6±23.9)	51±74 (31.8±22.1)	28±38 (22.6±24.0)	5±8[&§] (10.7±20.5) [&§]	0.007 (0.029)
Moraxella catarrhalis	0.8±1.1 (0.6±1.3)	1±2.2 (0.7±1.9)	0.1±0.3 (0.07±0.26)	0.2±0.7 (0.47±1.25)	0.567 (0.924)
Streptococcus pneumonae	0.06±0.13 (0.0±0.0)	0.0±0.0 (0.0±0.0)	0.11±0.34 (0.07±0.26)	0.0±0.0 (0.0±0.0)	0.710 (0.986)

Abbreviations: 16S=total bacterial load. The bacterial load (copies/ml) is normalized for bronchial biopsy superficial layer (mm^2). In brackets is the percentage of each bacterium studied over the total load value including *P. aeruginosa*+ *H. influenza*+ *M. catarrhalis*+ *S. pneumonia*. Data expressed as mean±Standard Error. Statistics: The Kruskal-Wallis test was used for multiple comparisons followed by Mann-Whitney U test for comparison between groups: *p<0.05, significantly different from control non-smokers; [&]p<0.05, significantly different from control smokers with normal lung function; [§]p<0.05, significantly different from mild/moderate COPD. The exact "p" values for comparison between groups are given in the Results section.

28

Figure Legends

Figure 1. Schematic representation of the molecular variations related to bacterial-related (panels a, b) molecules in the bronchial epithelium (panel a) and in the bronchial lamina propria (panel b) of control non-smokers, control smokers, mild/moderate stable COPD and severe/very severe stable COPD patients. With worsening of the disease, levels of TLR4 and NOD1 increase in bronchial epithelium (panel a) and in lamina propria (panel b). Panel (c) shows the *P. aeruginosa* and the *H. influenzae* variations in control subjects and in COPD patients of increasing severity. With worsening of the disease, levels of *P. aeruginosa* increase, while levels of *H. influenzae* decrease in bronchial biopsies. Panel (d) shows the TLR4 mRNA significant increase induced by H_2O_2 stimulation of bronchial epithelial cells (16HBE) at 2h after the oxidative stimulus. Data in panels a, b, c, d are expressed as median±Standard Error.

*significantly different from control non-smokers; [&]significantly different from control smokers; [§]significantly different from mild/moderate COPD. CNS=Control non-smokers; CS=Control smokers; M COPD=Mild/moderate COPD; S COPD=Severe/very severe COPD.

Figure 2. Regression analysis between TLR4 scored epithelial values and FEV1% predicted (panels a, c) and TLR4 scored epithelial values vs FEV1/FVC% (panels b, d). Correlations were performed in all smokers (panels a, b) and in patients with COPD alone (panels c, d). The lung functional indices of bronchial obstruction were significantly and inversely correlated to the immune expression of TLR4 in the bronchial epithelium of all smokers and of patients with COPD alone. Correlation coefficients were calculated using the Spearman rank method.

Figure 3. Regression analysis between FEV1% lung functional values and percentage of *P. aeruginosa* (panels a, c) and percentage of *H. influenzae* (panels b, d) in all smokers (panels a, b) and COPD patients (panels c, d). In the bronchial mucosa increased values of bronchial obstruction were associated to an increased percentage of *P. aeruginosa* in all smokers and a decreased percentage of *H. influenzae* in all smokers and patients with COPD. Correlation coefficients were calculated using the Spearman rank method.

Figure 4. *TLR4 and NOD1 signaling in COPD.* In the presence of concomitant oxidative stress stimuli, pathogen-associated molecular patterns (PAMPs) from micro-organisms

and endogenous molecules termed danger-associated molecular patterns (DAMPs) stimulate TLR4 leading to the recruitment of the TLR signaling adaptors myeloid differentiation primary response protein 88 (MYD88) and the adapter molecule toll-interleukin 1 receptor (TIR) domain containing adaptor protein (TIRAP). The MYD88 dependent pathway recruits the IL-1R-associated kinases (IRAKs) family of proteins which leads to IκB phosphorylation resulting in the activation and nuclear translocation of NF-κB which can be responsible for the over-expression of numerous inflammatory genes. TLR4, MYD88, TIRAP and p65 (NF-κB) result increased in COPD patients. Bacterial PG-derived peptides γ-D-glutamyl-m-diaminopimelic acid (iE-DAP) and muramyldipeptide (MDP) are recognized by the cytosolic receptors termed nucleotide-binding oligomerization domain (NOD)1 and NOD2. NOD1 and NOD2 through CARD-CARD interactions may stimulate downstream IKK complex which in turn, phosphorylates the NF-kB inhibitor IκBα followed by the NF-κB activation and nuclear translocation. Gram-negative bacteria preferentially activate NOD1 which was found up-regulated in our present study in COPD patients.

1

Supplementary material

Bronchial inflammation and bacterial load in stable COPD is associated with TLR4 overexpression

Antonino Di Stefano, PhD[1], Fabio LM Ricciardolo, MD, PhD[2], Gaetano Caramori MD, PhD[3], Ian M Adcock, PhD[4], Kian Fan Chung MD[4], Peter J Barnes MD[4], Paola Brun, PhD[5], Andrea Leonardi, MD[6], Filippo Andò MD[7], Davide Vallese, PhD[1], Isabella Gnemmi[1], Luisella Righi, MD[8], Francesco Cappello, MD[9,10], Bruno Balbi, MD[1]

Methods

Subjects

All COPD patients and control subjects who underwent bronchoscopy and bronchial biopsies were recruited from the Respiratory Medicine Unit of the Fondazione Salvatore Maugeri, Institute of Veruno (Veruno, Italy). In COPD patients, the severity of the airflow obstruction was graded using current GOLD criteria [http://goldcopd.org/]. All former smokers had stopped smoking for at least one year. COPD and chronic bronchitis were defined according to international guidelines, [http://goldcopd.org/]. COPD severity was graded according to international guidelines, [http://goldcopd.org/]. All COPD patients were stable with no previous exacerbation in the six months before bronchoscopy. None of the subjects were treated with theophylline, antibiotics, antioxidants, mucolytics, and/or glucocorticoids in the month prior bronchoscopy. COPD patients were using short-acting inhaled β2-agonists (SABA) or short-acting inhaled antimuscarinics (SAMA) prn or regular long-acting inhaled β2- agonists (LABA) and/or regular inhaled anticholinergics, including SAMA or long-acting inhaled antimuscarinics (LAMA) at the dosage recommended in current COPD guidelines [http://goldcopd.org/] at the time of their recruitment. The study conformed to the Declaration of Helsinki and was approved by the ethics committees of the (formerly) Fondazione Salvatore Maugeri, (formerly), at present: Istituti Clinici Scientifici Maugeri SpA, Società Benefit [Veruno (Novara), Italy], the University Hospital of Ferrara, Italy. Written informed consent was obtained from each subject and bronchial biopsies were performed according to the local ethic committee guidelines.

Lung function tests and volumes

1

2

Pulmonary function tests were performed as previously described (**E1**) according to guidelines recommendations. Pulmonary function tests included measurements of FEV_1 and FEV_1/FVC under baseline conditions in all the subjects examined (6200 Autobox Pulmonary Function Laboratory; Sensormedics Corp., Yorba Linda, CA, USA). In order to assess the reversibility of airflow obstruction and post bronchodilator functional values, the FEV_1 and $FEV_1/FVC\%$ measurements in the groups of subjects with $FEV_1/FVC\% \leq 70\%$ pre-bronchodilator was repeated 20 min after the inhalation of 0.4 mg of salbutamol.

Fiberoptic bronchoscopy and bronchial biopsy processing

Fiberoptic bronchoscopy, collection and processing of bronchial biopsies were performed as previously described (**E1**). In brief, four bronchial biopsy specimens were taken from segmental and subsegmental airways of the right lower and upper lobes using size 19 cupped forceps. Bronchial biopsies for immunohistochemistry were gently extracted from the forceps and processed for light microscopy as previously described (**E1**). At least two samples were embedded in Tissue Tek II OCT (Miles Scientific, Naperville, IL, USA), frozen within 15 min in isopentane pre-cooled in liquid nitrogen, and stored at –80°C. The best frozen sample was then oriented and 6μm thick cryostat sections were cut for immunohistochemical light microscopy analysis and processed as described below.

Immunohistochemistry analysis of TLRs and NLRs signaling pathways on bronchial biopsies

One cryostat section from each biopsy was stained with one each of a panel of primary antibodies specific for the inflammatory cells or signaling molecules studied (**Table E1**). Briefly, after blocking non-specific binding sites, primary antibody was applied at optimal dilutions and incubated for 1h at room temperature. Antibody binding was revealed with secondary anti-mouse (Vector, BA 2000), anti-rabbit (Vector, BA 1000) or anti-goat (Vector, BA 5000) antibodies followed by ABC kit AP AK5000, Vectastain and fast-red substrate (red color) or ABC kit HRP Elite, PK6100, Vectastain and diaminobenzidine (DAB) substrate (brown color). Human tonsil or nasal polyp were used as positive controls. For the negative controls, normal mouse, rabbit or goat non-specific immunoglobulins (Santa Cruz Biotechnology, Santa Cruz, CA, USA) were used at the same protein concentration as the primary antibody. Double staining for identification of CD8+, macrophages (CD68+) and endothelial cells (CD31+) co-expressing TLR4 and NOD1 was also performed; briefly, mouse monoclonal antibodies used for identification of CD8+,

2

3

CD68+ and CD31+ cells were revealed using the horse anti-mouse (Vector, BA 2000) followed by ABC kit AP AK 5000, Vectastain and fast-red substrate (red color). Rabbit or goat primary antibodies for identification of NOD1 (rabbit) and TLR4 (goat) were revealed using a goat anti rabbit (Vector, BA 1000) and a rabbit anti goat (Vector, BA 5000) antibodies followed by ABC kit HRP Elite, PK 6100, Vectastain and DAB substrate (brown color). For the negative controls, normal mouse, rabbit or goat non-specific immunoglobulins (Santa Cruz Biotechnology) were used at the same combination and protein concentration as the primary specific antibodies.

Scoring system for immunohistochemistry
Morphometric measurements were performed with a light microscope (Leitz Biomed, Leica Cambridge, UK) connected to a video recorder linked to a computerized image system (Quantimet 500 Image Processing and Analysis System, Software Qwin V0200B, Leica). Light-microscopic analysis was performed at a magnification of 630x. The immunostaining for all the antigens studied was scored (range: 0 = absence of immunostaining to 3 = extensive intense immunostaining) in the intact (columnar and basal epithelial cells) bronchial epithelium, as previously described (**E1**). The final result was expressed as the average of all scored fields obtained from each biopsy. A mean±SD of 0.70±0.26 millimeters of epithelium was analyzed in COPD patients and control subjects. A minimum length of 450 microns of intact epithelium was studied for each patient.

Immunostained cells in bronchial submucosa (lamina propria) were quantified 100-μm beneath the epithelial basement membrane in several non-overlapping high-power fields until the whole specimen was examined. The final result, expressed as the number of positive cells per square millimeter, was calculated as the average of all the cellular counts performed in each biopsy.

Quantification of the bacterial load in the bronchial biopsies
qRT-PCR was used to quantify the 16S ribosomal subunit (total bacterial load) and the genome copy number (copies/ml) per mm^2 of bronchial tissue examined of *Pseudomonas aeruginosa (P. aeruginosa), Haemophilus ~~influenzae~~influenza (H. influenza), Moraxella catarrhalis (M. catarrhalis)* and *Streptococcus ~~pneumoniae~~pneumonia (S. pneumoniae)*. In brief, total bacterial DNA was extracted under sterile conditions from 30μm cryostat sections of bronchial biopsies using the QIAmp DNA Mini Kit (Cat. # 56304, Qiagen) following the manufacturer's instructions and re-suspended in 100μl nuclease-free water.

3

1
2
3
4
5
6
7
8
9
10
11
12
13
14
15
16
17
18
19
20
21
22
23
24
25
26
27
28
29
30
31
32
33
34
35
36
37
38
39
40
41
42
43
44
45
46
47
48
49
50
51
52
53
54
55
56
57
58
59
60

4

DNA was stored at −20°C before amplification. DNA standards for qRT-PCR were prepared from pure DNA cultures of *Escherichia coli, H. influenzae, M. catarrhalis, P. aeruginosa, and S. pneumoniae* and were used to generate standard curves. The standard curves were always performed in triplicate with regression coefficients close to 1 (range of R^2 values: 0.984-0.994 for *E. coli*, 0.986-0.999 for *H. influenzae*, 0.990-0.998 for *M. catarrhalis*, 0.987-0.999 for *P. aeruginosa* and 0.984-0.997 for *S. pneumoniae*) and showed a linear increase within the range of DNA concentration utilized.

Primers for the specific amplification of *H. influenzae, M. catarrhalis, P. aeruginosa,* and *S. pneumoniae* were synthesized by Life Technologies (Milan, Italy) and are shown in **Table E2**. DNA amplification and detection were performed in a Rotor Gene Q system (Qiagen) using the QuantiFastTM SYBER Green PCR Kit (Cat. # 204054, Qiagen). RT-PCR cycling conditions were: 95°C for 5 min (PCR initial activation step); 40 amplification cycles of 95°C for 5 s (denaturation) and 60°C for 10 s (combined annealing/extension), followed by melting curve analysis to ensure the specificity of the PCR amplification. For each reaction, negative controls were run in triplicate, consisting of primers, PCR Mastermix and sterile water instead of DNA template. Amplification, data acquisition, and cycle threshold (CT) values analysis were performed using the Rotor Gene Q software (Rotor-Gene Q Series Software 2.0.2). For each patient and control subject, an adjacent 6μm cryostat section, stained with H&E, was used for measurement of the sub-epithelial basement membrane length. All data were expressed as number of bacterial DNA copies/ml normalized for the sub-epithelial basement membrane length multiplied by the cryostat section thickness (30μm), corresponding to the square millimeters (mm^2) of the more superficial layer of bronchial tissue examined for each subject.

Cell Culture and Treatments

The 16HBE human epithelial cell line was grown in Dulbecco's modified Minimum Essential Medium (DMEM), supplemented with 10% v/v fetal bovine serum (FBS), 50 IU/ml penicillin, 50μg/ml streptomycin, 1x non-essential amino acids, 1mM sodium pyruvate and 2mM glutamine (37°C, 5% CO_2). When cells were at 60-70% confluent, the medium was replaced with supplemented DMEM without FBS for starvation time (24h), followed by supplemented DMEM plus 1% FBS in the absence or presence of H_2O_2 (100μM) for 2, 4 ,8, 16 and 24 hours. All experiments were performed at least four times (in quadruplicate).

4

1
2
3
4
5
6
7
8
9
10
11
12
13
14
15
16
17
18
19
20
21
22
23
24
25
26
27
28
29
30
31
32
33
34
35
36
37
38
39
40
41
42
43
44
45
46
47
48
49
50
51
52
53
54
55
56
57
58
59
60

5

Extraction and Quantification of RNA and qRT-PCR from 16HBE

Total cellular RNA from treated and non-treated cultures was purified and isolated, using RNAspin Mini RNA Isolation kit (GE Healthcare, Buckinghamshire, UK) following the manufacturer's instructions. Total RNA was re-suspended in 100μl nuclease-free water and RNA concentration determined by spectroscopy (λ260/280 nm, Eppendorf BioPhotometer plus), and stored at -80–°C until use. Gene expression was measured using the Syber green for qRT-PCR in a Rotor Gene Q (Qiagen) system. One-step real-time PCR was carried out by amplifying mRNA using the QuantiFastTM SYBER Green RT-PCR Kit (Qiagen), according to the manufacturer's instructions, and gene specific primers (Qiagen) for TLR4 (Cat. # QT01670123, Qiagen) and glyceraldehyde-3-phosphate dehydrogenase (GAPDH) (Cat # QT01192646). Cycle threshold (CT) values were determined using the Rotor Gene Q software (Rotor-Gene Q Series Software 2.0.2). The expression levels of all genes studied were normalized to GAPDH levels in each sample to determine the expression between treated and non-treated cells using the $2^{-\Delta\Delta Ct}$ method (**E2**).

Statistical analysis

Group data were expressed as mean (standard deviation) for functional data and median (range) or interquartile range (IQR) for morphologic data. Differences between groups were analyzed using analysis of variance (ANOVA) for functional data. The ANOVA test was followed by the unpaired t-test for comparison between groups. The Kruskal-Wallis test applied for morphologic data was followed by the Mann-Whitney U test for comparison between groups. Correlation coefficients were calculated using the Spearman rank method. Probability values of $p<0.05$ were considered significant. Data analysis was performed using the Stat View SE Graphics program (Abacus Concepts Inc., Berkeley, CA, USA).

5

1
2
3
4
5
6
7
8
9
10
11
12
13
14
15
16
17
18
19
20
21
22
23
24
25
26
27
28
29
30
31
32
33
34
35
36
37
38
39
40
41
42
43
44
45
46
47
48
49
50
51
52
53
54
55
56
57
58
59
60

6

Table E1 Primary antibodies and immunohistochemical conditions used for identification of innate immune proteins, cytokines and inflammatory cells.

Target	Supplier	Cat.#[a]	Source	Dilution	Positive control
TLR2	Serotec	AHP1424	rabbit	1:300	Nasal polyp, tonsil
TLR4	R&D	AF1478	goat	1:80	Nasal polyp, tonsil
TLR9	Serotec	AHP1823	goat	1:150	Nasal polyp, tonsil
CD14	Sigma	C7673	mouse	1:40	Nasal polyp, tonsil
NOD1	Novus Biol.	NBP131349	rabbit	1:300	Nasal polyp, tonsil
NOD2	Santa Cruz	Sc-56168	mouse	1:25	Nasal polyp, tonsil
MYD88	Santa Cruz	Sc-11356	rabbit	1:150	Nasal polyp, tonsil
TIRAP	Serotec	AHP866T	rabbit	1:300	Nasal polyp, tonsil
Phospho-IRAK1	Santa Cruz	Sc-130197	rabbit	1:50	Nasal polyp, tonsil
IRAK4	R&D	AF3919	goat	1:300	Nasal polyp, tonsil
CD4	Dako	M716	Mouse	1:100	tonsil
CD8	Dako	M7103	Mouse	1:200	tonsil
CD68	Dako	M814	Mouse	1:200	tonsil
CD31	Dako	M823	Mouse	1:40	Nasal polyp
Neutrophil elastase	Dako	M752	Mouse	1:100	Nasal polyp

[a]Cat#, catalogue number; (p): paraffin embedded peripheral lung tissue pretreated with citrate buffer (pH 6) and microwave exposure. See methods section for details

6

7

Table E2. List of primers used for qRT-PCR of bacteria in the study of bronchial biopsies

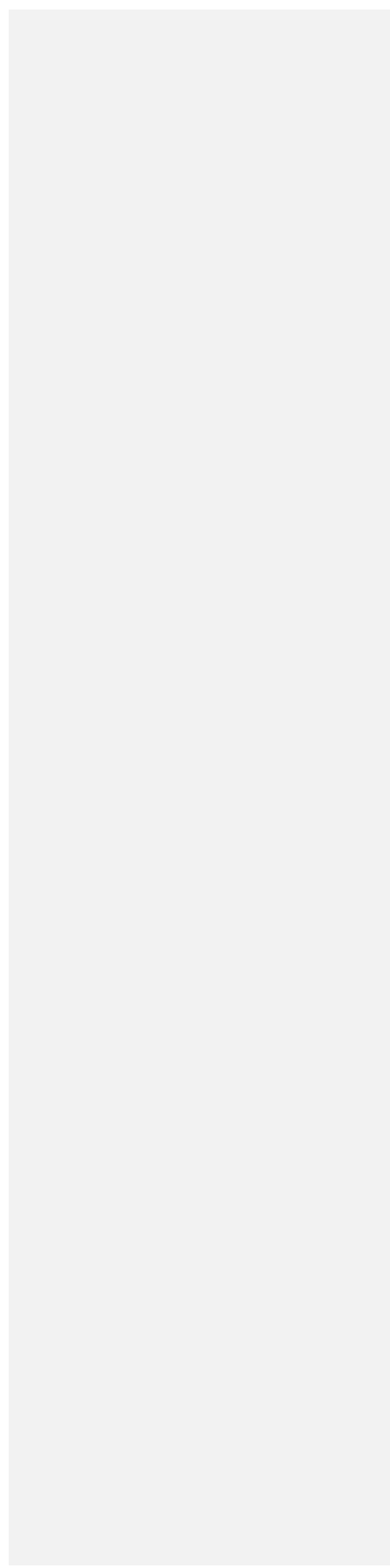| Primer type	Primer	Sequence (5' to 3')	Reference
16S rRNA	*Eub-F*	F: 5'-TCCTACGGGAGGCAGCAGT-3'	*Nadkarni, 2002[a]*
	Eub-R	R:5'-GGACTACCAGGGTATCTAATCCTGTT-3'	*Nadkarni, 2002[a]*
Escherichia coli	*E.coli F*	F: 5'-CATGCCGCGTGTATGAAGAA-3'	*Huijsdens, ~~X.W.~~, 2002[b]*
	E.coli R	R: 5'-CGGGTAACGTCAATGAGCAAA-3'	*Huijsdens, ~~X.W.~~, 2002[b]*
Haemophilus influenzae	*HelS-F*	F: 5'-CCGGGTGCGGTAGAATTTAATAA-3'	*Rogers GB, 2014[c]*
	Eub-R	R: 5'-CTGATTTTTCAGTGCTGTCTTTGC-3'	*Rogers GB, 2014[c]*
Moraxella catarrhalis	*copB-F*	F: 5'-GTGAGTGCCGCTTTTACAACC-3'	*Sethi S, 1997[d]*
	copB-R	R: 5'-TGTATCGCCTGCCAAGACAA-3'	*Sethi S,1997[d]*
Pseudomonas aeruginosa	*gyrB-F*	F: 5'-CCTGACCATCCGTCGCCACAAC-3'	*Qin X, 2003[e]*
	gyrB-R	R: 5'-CGCAGCAGGATGCCGACGCC-3'	*Qin X, 2003[e]*
Streptococcus pneumoniae	*Spn9802-F*	F: 5'-AGTCGTTCCAAGGTAACAAGTCT-3'	*Abdeldaim ~~GM~~, 2008[f]*
	Spn9802-R	R: 5'-ACCAACTCGACCACCTCTTT-3'	*Abdeldaim ~~GM~~, 2008[f]*

References: a) Nadkarni MA, Martin FE, Jacques NA, Hunter N. Determination of bacterial load by real-time PCR using a broad-range (universal) probe and primers set. Microbiology. 2002;148(Pt 1):257-66. b) Huijsdens XW, Linskens RK, Mak M, Meuwissen SG, Vandenbroucke-Grauls CM, Savelkoul PH. Quantification of bacteria adherent to gastrointestinal mucosa by real-time PCR. J Clin Microbiol. 2002;40(12):4423-7. c) Rogers GB, Zain NM, Bruce KD, Burr LD, Chen AC, Rivett DW, McGuckin MA, Serisier DJ. A novel microbiota stratification system predicts future exacerbations in bronchiectasis. Ann Am Thorac Soc. 2014;11(4):496-503. d) Sethi S, Surface JM, Murphy TF. Antigenic heterogeneity and molecular analysis of CopB of Moraxella (Branhamella) catarrhalis. Infect Immun. 1997;65(9):3666-71. e) Qin X, Emerson J, Stapp J, Stapp L, Abe P, Burns JL. Use of real-time PCR with multiple targets to identify Pseudomonas aeruginosa and other nonfermenting gram-negative bacilli from patients with cystic fibrosis. J Clin Microbiol. 2003;41(9):4312-7. f) Abdeldaim GM, Strålin K, Olcén P, Blomberg J, Herrmann B. Toward a quantitative DNA-based definition of pneumococcal pneumonia: a comparison

7

1
2
3
4
5
6
7
8
9
10
11
12
13
14
15
16
17
18
19
20
21
22
23
24
25
26
27
28
29
30
31
32
33
34
35
36
37
38
39
40
41
42
43
44
45
46
47
48
49
50
51
52
53
54
55
56
57
58
59
60

8

of Streptococcus pneumoniae target genes, with special reference to the Spn9802 fragment. Diagn Microbiol Infect Dis. 2008;60(2):143-50.

8

9

E-Figure legends

Figure E1. Photomicrographs showing the bronchial mucosa from control non-smokers (panel a), Control smokers with normal lung function (panel b), mild/moderate COPD (panel c) and severe/very severe COPD patients (panel d) immune-stained (arrows indicate some immunopositive cells) for identification of TLR4 in the bronchial epithelium and lamina propria. Results are representative of those from 12 non-smokers, 12 smokers with normal lung function, 16 mild/moderate COPD and 18 severe/very severe COPD patients. Negative control immunostaining, performed in a nasal polyp section, including an irrelevant goat primary antibody (not shown). Bar=30 microns.

Figure E2. Photomicrographs showing the bronchial mucosa from control non-smokers (panel a), Control smokers with normal lung function (panel b), mild/moderate COPD (panel c) and severe/very severe COPD patients (panel d) immune-stained (arrows indicate some immunopositive cells) for identification of NOD1 in the bronchial epithelium and lamina propria. Results are representative of those from 12 non-smokers, 12 smokers with normal lung function, 16 mild/moderate COPD and 18 severe/very severe COPD patients. Negative control immunostaining, performed in a nasal polyp section, including an irrelevant rabbit primary antibody (not shown). Bar=30 microns.

Figure E3. Photomicrographs showing the bronchial mucosa from severe COPD patients double-immunostained for identification of CD8+ (a, d), CD68+ (b, e) and CD31+ (c, f) cells (red-colour) co-expressing TLR4 (a, b, c, respectively) (brown-colour) and NOD1 (d, e, f, respectively) (brown-colour) in the bronchial lamina propria. TLR4 and NOD1 were revealed by diaminobenzidine substrate, whereas inflammatory cells (CD8+, CD68+) and endothelial cells (CD31+) were revealed using fast red substrate. Arrows indicate double-stained cells. Bar=15 microns.

9

10

E-References

E1. **Di Stefano A, Caramori G, Barczyk A, Vicari C, Brun P, Zanini A, Cappello F, Garofano E, Padovani A, Contoli M, Casolari P, Durham AL, Chung KF, Barnes PJ, Papi A, Adcock I, Balbi B.** Innate immunity but not NLRP3 inflammasome activation correlates with severity of stable COPD. Thorax. 2014;69:516-524.

E2. **Livak KJ, Schmittgen TD.** Analysis of relative gene expression data using real-time quantitative PCR and the 2(-Delta Delta C(T)) Method. Methods. 2001;25:402-408.

Supplementary material

Bronchial inflammation and bacterial load in stable COPD is associated with TLR4 overexpression

Antonino Di Stefano, PhD[1], Fabio LM Ricciardolo, MD, PhD[2], Gaetano Caramori MD, PhD[3], Ian M Adcock, PhD[4], Kian Fan Chung MD[4], Peter J Barnes MD[4], Paola Brun, PhD[5], Andrea Leonardi, MD[6], Filippo Andò MD[7], Davide Vallese, PhD[1], Isabella Gnemmi[1], Luisella Righi, MD[8], Francesco Cappello, MD[9,10], Bruno Balbi, MD[1]

Methods

Subjects

All COPD patients and control subjects who underwent bronchoscopy and bronchial biopsies were recruited from the Respiratory Medicine Unit of the Fondazione Salvatore Maugeri, Institute of Veruno (Veruno, Italy). In COPD patients, the severity of the airflow obstruction was graded using current GOLD criteria [http://goldcopd.org/]. All former smokers had stopped smoking for at least one year. COPD and chronic bronchitis were defined according to international guidelines, [http://goldcopd.org/]. COPD severity was graded according to international guidelines, [http://goldcopd.org/]. All COPD patients were stable with no previous exacerbation in the six months before bronchoscopy. None of the subjects were treated with theophylline, antibiotics, antioxidants, mucolytics, and/or glucocorticoids in the month prior bronchoscopy. COPD patients were using short-acting inhaled β2-agonists (SABA) or short-acting inhaled antimuscarinics (SAMA) prn or regular long-acting inhaled β2- agonists (LABA) and/or regular inhaled anticholinergics, including SAMA or long-acting inhaled antimuscarinics (LAMA) at the dosage recommended in current COPD guidelines [http://goldcopd.org/] at the time of their recruitment. The study conformed to the Declaration of Helsinki and was approved by the ethics committees of the (formerly) Fondazione Salvatore Maugeri, at present: Istituti Clinici Scientifici Maugeri SpA, Società Benefit [Veruno (Novara), Italy, the University Hospital of Ferrara, Italy. Written informed consent was obtained from each subject and bronchial biopsies were performed according to the local ethic committee guidelines.

Lung function tests and volumes

Pulmonary function tests were performed as previously described (**E1**) according to guidelines recommendations. Pulmonary function tests included measurements of FEV_1 and FEV_1/FVC under baseline conditions in all the subjects examined (6200 Autobox Pulmonary Function Laboratory; Sensormedics Corp., Yorba Linda, CA, USA). In order to assess the reversibility of airflow obstruction and post bronchodilator functional values, the FEV_1 and $FEV_1/FVC\%$ measurements in the groups of subjects with $FEV_1/FVC\% \leq 70\%$ pre-bronchodilator was repeated 20 min after the inhalation of 0.4 mg of salbutamol.

Fiberoptic bronchoscopy and bronchial biopsy processing

Fiberoptic bronchoscopy, collection and processing of bronchial biopsies were performed as previously described (**E1**). In brief, four bronchial biopsy specimens were taken from segmental and subsegmental airways of the right lower and upper lobes using size 19 cupped forceps. Bronchial biopsies for immunohistochemistry were gently extracted from the forceps and processed for light microscopy as previously described (**E1**). At least two samples were embedded in Tissue Tek II OCT (Miles Scientific, Naperville, IL, USA), frozen within 15 min in isopentane pre-cooled in liquid nitrogen, and stored at –80°C. The best frozen sample was then oriented and 6μm thick cryostat sections were cut for immunohistochemical light microscopy analysis and processed as described below.

Immunohistochemistry analysis of TLRs and NLRs signaling pathways on bronchial biopsies

One cryostat section from each biopsy was stained with one each of a panel of primary antibodies specific for the inflammatory cells or signaling molecules studied (**Table E1**). Briefly, after blocking non-specific binding sites, primary antibody was applied at optimal dilutions and incubated for 1h at room temperature. Antibody binding was revealed with secondary anti-mouse (Vector, BA 2000), anti-rabbit (Vector, BA 1000) or anti-goat (Vector, BA 5000) antibodies followed by ABC kit AP AK5000, Vectastain and fast-red substrate (red color) or ABC kit HRP Elite, PK6100, Vectastain and diaminobenzidine (DAB) substrate (brown color). Human tonsil or nasal polyp were used as positive controls. For the negative controls, normal mouse, rabbit or goat non-specific immunoglobulins (Santa Cruz Biotechnology, Santa Cruz, CA, USA) were used at the same protein concentration as the primary antibody. Double staining for identification of CD8+, macrophages (CD68+) and endothelial cells (CD31+) co-expressing TLR4 and NOD1 was also performed; briefly, mouse monoclonal antibodies used for identification of CD8+,

CD68+ and CD31+ cells were revealed using the horse anti-mouse (Vector, BA 2000) followed by ABC kit AP AK 5000, Vectastain and fast-red substrate (red color). Rabbit or goat primary antibodies for identification of NOD1 (rabbit) and TLR4 (goat) were revealed using a goat anti rabbit (Vector, BA 1000) and a rabbit anti goat (Vector, BA 5000) antibodies followed by ABC kit HRP Elite, PK 6100, Vectastain and DAB substrate (brown color). For the negative controls, normal mouse, rabbit or goat non-specific immunoglobulins (Santa Cruz Biotechnology) were used at the same combination and protein concentration as the primary specific antibodies.

Scoring system for immunohistochemistry

Morphometric measurements were performed with a light microscope (Leitz Biomed, Leica Cambridge, UK) connected to a video recorder linked to a computerized image system (Quantimet 500 Image Processing and Analysis System, Software Qwin V0200B, Leica). Light-microscopic analysis was performed at a magnification of 630x. The immunostaining for all the antigens studied was scored (range: 0 = absence of immunostaining to 3 = extensive intense immunostaining) in the intact (columnar and basal epithelial cells) bronchial epithelium, as previously described (**E1**). The final result was expressed as the average of all scored fields obtained from each biopsy. A mean±SD of 0.70±0.26 millimeters of epithelium was analyzed in COPD patients and control subjects. A minimum length of 450 microns of intact epithelium was studied for each patient.

Immunostained cells in bronchial submucosa (lamina propria) were quantified $100\mu m$ beneath the epithelial basement membrane in several non-overlapping high-power fields until the whole specimen was examined. The final result, expressed as the number of positive cells per square millimeter, was calculated as the average of all the cellular counts performed in each biopsy.

Quantification of the bacterial load in the bronchial biopsies

qRT-PCR was used to quantify the 16S ribosomal subunit (total bacterial load) and the genome copy number (copies/ml) per mm^2 of bronchial tissue examined of *Pseudomonas aeruginosa (P. aeruginosa), Haemophilus influenza (H. influenza), Moraxella catarrhalis (M. catarrhalis)* and *Streptococcus pneumonia (S. pneumoniae).* In brief, total bacterial DNA was extracted under sterile conditions from 30µm cryostat sections of bronchial biopsies using the QIAmp DNA Mini Kit (Cat. # 56304, Qiagen) following the manufacturer's instructions and re-suspended in 100µl nuclease-free water. DNA was

stored at −20°C before amplification. DNA standards for qRT-PCR were prepared from pure DNA cultures of *Escherichia coli, H. influenzae, M. catarrhalis, P. aeruginosa, and S. pneumoniae* and were used to generate standard curves. The standard curves were always performed in triplicate with regression coefficients close to 1 (range of R^2 values: 0.984-0.994 for *E. coli*, 0.986-0.999 for *H. influenzae*, 0.990-0.998 for *M. catarrhalis*, 0.987-0.999 for *P. aeruginosa* and 0.984-0.997 for *S. pneumoniae*) and showed a linear increase within the range of DNA concentration utilized.

Primers for the specific amplification of *H. influenzae, M. catarrhalis, P. aeruginosa,* and *S. pneumoniae* were synthesized by Life Technologies (Milan, Italy) and are shown in **Table E2**. DNA amplification and detection were performed in a Rotor Gene Q system (Qiagen) using the QuantiFastTM SYBER Green PCR Kit (Cat. # 204054, Qiagen). RT-PCR cycling conditions were: 95°C for 5 min (PCR initial activation step); 40 amplification cycles of 95°C for 5 s (denaturation) and 60°C for 10 s (combined annealing/extension), followed by melting curve analysis to ensure the specificity of the PCR amplification. For each reaction, negative controls were run in triplicate, consisting of primers, PCR Mastermix and sterile water instead of DNA template. Amplification, data acquisition, and cycle threshold (CT) values analysis were performed using the Rotor Gene Q software (Rotor-Gene Q Series Software 2.0.2). For each patient and control subject, an adjacent 6μm cryostat section, stained with H&E, was used for measurement of the sub-epithelial basement membrane length. All data were expressed as number of bacterial DNA copies/ml normalized for the sub-epithelial basement membrane length multiplied by the cryostat section thickness (30μm), corresponding to the square millimeters (mm^2) of the more superficial layer of bronchial tissue examined for each subject.

Cell Culture and Treatments

The 16HBE human epithelial cell line was grown in Dulbecco's modified Minimum Essential Medium (DMEM), supplemented with 10% v/v fetal bovine serum (FBS), 50 IU/ml penicillin, 50μg/ml streptomycin, 1x non-essential amino acids, 1mM sodium pyruvate and 2mM glutamine (37°C, 5% CO_2). When cells were at 60-70% confluent, the medium was replaced with supplemented DMEM without FBS for starvation time (24h), followed by supplemented DMEM plus 1% FBS in the absence or presence of H_2O_2 (100μM) for 2, 4 ,8, 16 and 24 hours. All experiments were performed at least four times (in quadruplicate).

1
2
3
4
5
6
7
8
9
10
11
12
13
14
15
16
17
18
19
20
21
22
23
24
25
26
27
28
29
30
31
32
33
34
35
36
37
38
39
40
41
42
43
44
45
46
47
48
49
50
51
52
53
54
55
56
57
58
59
60

Extraction and Quantification of RNA and qRT-PCR from 16HBE

Total cellular RNA from treated and non-treated cultures was purified and isolated, using RNAspin Mini RNA Isolation kit (GE Healthcare, Buckinghamshire, UK) following the manufacturer's instructions. Total RNA was re-suspended in 100µl nuclease-free water and RNA concentration determined by spectroscopy (λ260/280 nm, Eppendorf BioPhotometer plus), and stored at -80°C until use. Gene expression was measured using the Syber green for qRT-PCR in a Rotor Gene Q (Qiagen) system. One-step real-time PCR was carried out by amplifying mRNA using the QuantiFastTM SYBER Green RT-PCR Kit (Qiagen), according to the manufacturer's instructions, and gene specific primers (Qiagen) for TLR4 (Cat. # QT01670123, Qiagen) and glyceraldehyde-3-phosphate dehydrogenase (GAPDH) (Cat # QT01192646). Cycle threshold (CT) values were determined using the Rotor Gene Q software (Rotor-Gene Q Series Software 2.0.2). The expression levels of all genes studied were normalized to GAPDH levels in each sample to determine the expression between treated and non-treated cells using the $2^{-\Delta\Delta Ct}$ method (**E2**).

Statistical analysis

Group data were expressed as mean (standard deviation) for functional data and median (range) or interquartile range (IQR) for morphologic data. Differences between groups were analyzed using analysis of variance (ANOVA) for functional data. The ANOVA test was followed by the unpaired t-test for comparison between groups. The Kruskal-Wallis test applied for morphologic data was followed by the Mann-Whitney U test for comparison between groups. Correlation coefficients were calculated using the Spearman rank method. Probability values of $p<0.05$ were considered significant. Data analysis was performed using the Stat View SE Graphics program (Abacus Concepts Inc., Berkeley, CA, USA).

6

1
2
3
4
5
6
7
8
9
10
11
12
13
14
15
16
17
18
19
20
21
22
23
24
25
26
27
28
29
30
31
32
33
34
35
36
37
38
39
40
41
42
43
44
45
46
47
48
49
50
51
52
53
54
55
56
57
58
59
60

Table E1 Primary antibodies and immunohistochemical conditions used for identification of innate immune proteins, cytokines and inflammatory cells.

Target	Supplier	Cat.#[a]	Source	Dilution	Positive control
TLR2	Serotec	AHP1424	rabbit	1:300	Nasal polyp, tonsil
TLR4	R&D	AF1478	goat	1:80	Nasal polyp, tonsil
TLR9	Serotec	AHP1823	goat	1:150	Nasal polyp, tonsil
CD14	Sigma	C7673	mouse	1:40	Nasal polyp, tonsil
NOD1	Novus Biol.	NBP131349	rabbit	1:300	Nasal polyp, tonsil
NOD2	Santa Cruz	Sc-56168	mouse	1:25	Nasal polyp, tonsil
MYD88	Santa Cruz	Sc-11356	rabbit	1:150	Nasal polyp, tonsil
TIRAP	Serotec	AHP866T	rabbit	1:300	Nasal polyp, tonsil
Phospho-IRAK1	Santa Cruz	Sc-130197	rabbit	1:50	Nasal polyp, tonsil
IRAK4	R&D	AF3919	goat	1:300	Nasal polyp, tonsil
CD4	Dako	M716	Mouse	1:100	tonsil
CD8	Dako	M7103	Mouse	1:200	tonsil
CD68	Dako	M814	Mouse	1:200	tonsil
CD31	Dako	M823	Mouse	1:40	Nasal polyp
Neutrophil elastase	Dako	M752	Mouse	1:100	Nasal polyp

[a]Cat#, catalogue number; (p): paraffin embedded peripheral lung tissue pretreated with citrate buffer (pH 6) and microwave exposure. See methods section for details

Table E2. List of primers used for qRT-PCR of bacteria in the study of bronchial biopsies

Primer type	Primer	Sequence (5' to 3')	Reference
16S rRNA	Eub-F	F: 5'-TCCTACGGGAGGCAGCAGT-3'	Nadkarni, 2002[a]
	Eub-R	R:5'-GGACTACCAGGGTATCTAATCCTGTT-3'	Nadkarni, 2002[a]
Escherichia coli	E.coli F	F: 5'-CATGCCGCGTGTATGAAGAA-3'	Huijsdens, 2002[b]
	E.coli R	R: 5'-CGGGTAACGTCAATGAGCAAA-3'	Huijsdens, 2002[b]
Haemophilus influenzae	HelS-F	F: 5'-CCGGGTGCGGTAGAATTTAATAA-3'	Rogers GB, 2014[c]
	Eub-R	R: 5'-CTGATTTTTCAGTGCTGTCTTTGC-3'	Rogers GB, 2014[c]
Moraxella catarrhalis	copB-F	F: 5'-GTGAGTGCCGCTTTTACAACC-3'	Sethi S, 1997[d]
	copB-R	R: 5'-TGTATCGCCTGCCAAGACAA-3'	Sethi S,1997[d]
Pseudomonas aeruginosa	gyrB-F	F: 5'-CCTGACCATCCGTCGCCACAAC-3'	Qin X, 2003[e]
	gyrB-R	R: 5'-CGCAGCAGGATGCCGACGCC-3'	Qin X, 2003[e]
Streptococcus pneumoniae	Spn9802-F	F: 5'-AGTCGTTCCAAGGTAACAAGTCT-3'	Abdeldaim, 2008[f]
	Spn9802-R	R: 5'-ACCAACTCGACCACCTCTTT-3'	Abdeldaim, 2008[f]

References: a) Nadkarni MA, Martin FE, Jacques NA, Hunter N. Determination of bacterial load by real-time PCR using a broad-range (universal) probe and primers set. Microbiology. 2002;148(Pt 1):257-66. b) Huijsdens XW, Linskens RK, Mak M, Meuwissen SG, Vandenbroucke-Grauls CM, Savelkoul PH. Quantification of bacteria adherent to gastrointestinal mucosa by real-time PCR. J Clin Microbiol. 2002;40(12):4423-7. c) Rogers GB, Zain NM, Bruce KD, Burr LD, Chen AC, Rivett DW, McGuckin MA, Serisier DJ. A novel microbiota stratification system predicts future exacerbations in bronchiectasis. Ann Am Thorac Soc. 2014;11(4):496-503. d) Sethi S, Surface JM, Murphy TF. Antigenic heterogeneity and molecular analysis of CopB of Moraxella (Branhamella) catarrhalis. Infect Immun. 1997;65(9):3666-71. e) Qin X, Emerson J, Stapp J, Stapp L, Abe P, Burns JL. Use of real-time PCR with multiple targets to identify Pseudomonas aeruginosa and other nonfermenting gram-negative bacilli from patients with cystic fibrosis. J Clin Microbiol. 2003;41(9):4312-7. f) Abdeldaim GM, Strålin K, Olcén P, Blomberg J, Herrmann B. Toward a quantitative DNA-based definition of pneumococcal pneumonia: a comparison of Streptococcus pneumoniae target genes, with special reference to the Spn9802 fragment. Diagn Microbiol Infect Dis. 2008;60(2):143-50.

E-Figure legends

Figure E1. Photomicrographs showing the bronchial mucosa from control non-smokers (panel a), Control smokers with normal lung function (panel b), mild/moderate COPD (panel c) and severe/very severe COPD patients (panel d) immune-stained (arrows indicate some immunopositive cells) for identification of TLR4 in the bronchial epithelium and lamina propria. Results are representative of those from 12 non-smokers, 12 smokers with normal lung function, 16 mild/moderate COPD and 18 severe/very severe COPD patients. Negative control immunostaining, performed in a nasal polyp section, including an irrelevant goat primary antibody (not shown). Bar=30 microns.

Figure E2. Photomicrographs showing the bronchial mucosa from control non-smokers (panel a), Control smokers with normal lung function (panel b), mild/moderate COPD (panel c) and severe/very severe COPD patients (panel d) immune-stained (arrows indicate some immunopositive cells) for identification of NOD1 in the bronchial epithelium and lamina propria. Results are representative of those from 12 non-smokers, 12 smokers with normal lung function, 16 mild/moderate COPD and 18 severe/very severe COPD patients. Negative control immunostaining, performed in a nasal polyp section, including an irrelevant rabbit primary antibody (not shown). Bar=30 microns.

Figure E3. Photomicrographs showing the bronchial mucosa from severe COPD patients double-immunostained for identification of CD8+ (a, d), CD68+ (b, e) and CD31+ (c, f) cells (red-colour) co-expressing TLR4 (a, b, c, respectively) (brown-colour) and NOD1 (d, e, f, respectively) (brown-colour) in the bronchial lamina propria. TLR4 and NOD1 were revealed by diaminobenzidine substrate, whereas inflammatory cells (CD8+, CD68+) and endothelial cells (CD31+) were revealed using fast red substrate. Arrows indicate double-stained cells. Bar=15 microns.

1
2
3
4
5
6
7
8
9
10
11
12
13
14
15
16
17
18
19
20
21
22
23
24
25
26
27
28
29
30
31
32
33
34
35
36
37
38
39
40
41
42
43
44
45
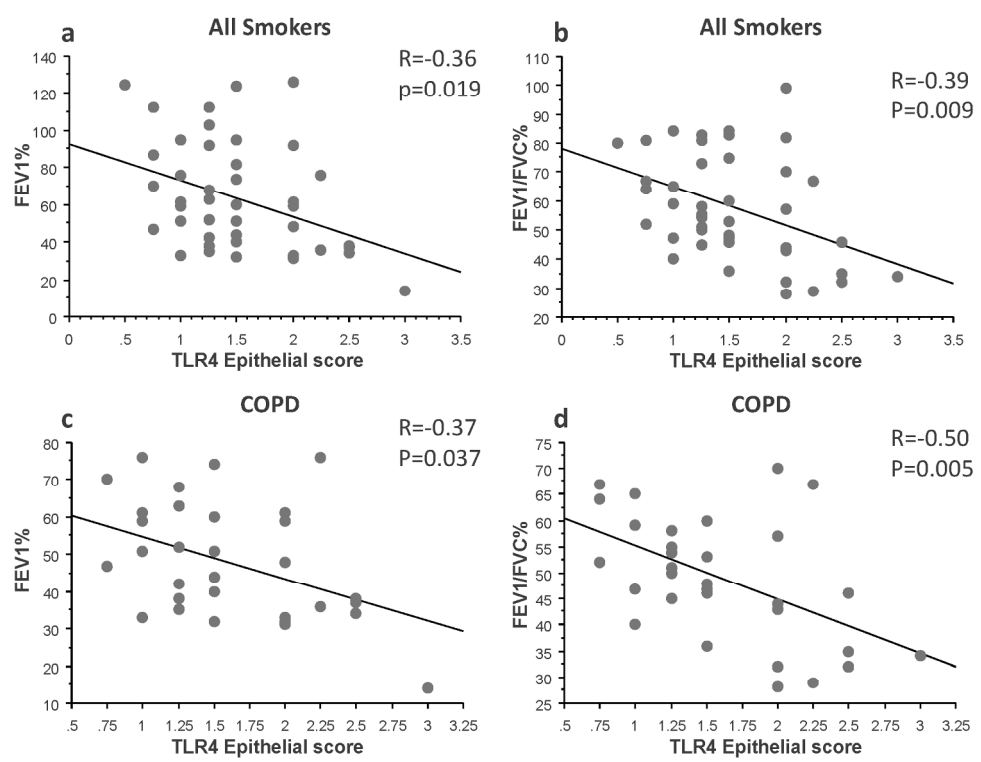46
47
48
49
50
51
52
53
54
55
56
57
58
59
60

E-References

E1**. Di Stefano A, Caramori G, Barczyk A, Vicari C, Brun P, Zanini A, Cappello F, Garofano E, Padovani A, Contoli M, Casolari P, Durham AL, Chung KF, Barnes PJ, Papi A, Adcock I, Balbi B.** Innate immunity but not NLRP3 inflammasome activation correlates with severity of stable COPD. Thorax. 2014;69:516-524.

E2. **Livak KJ, Schmittgen TD.** Analysis of relative gene expression data using real-time quantitative PCR and the 2(-Delta Delta C(T)) Method. Methods. 2001;25:402-408.

figure 1
figure 1
263x195mm (300 x 300 DPI)

figure 2
figure 2
194x151mm (300 x 300 DPI)
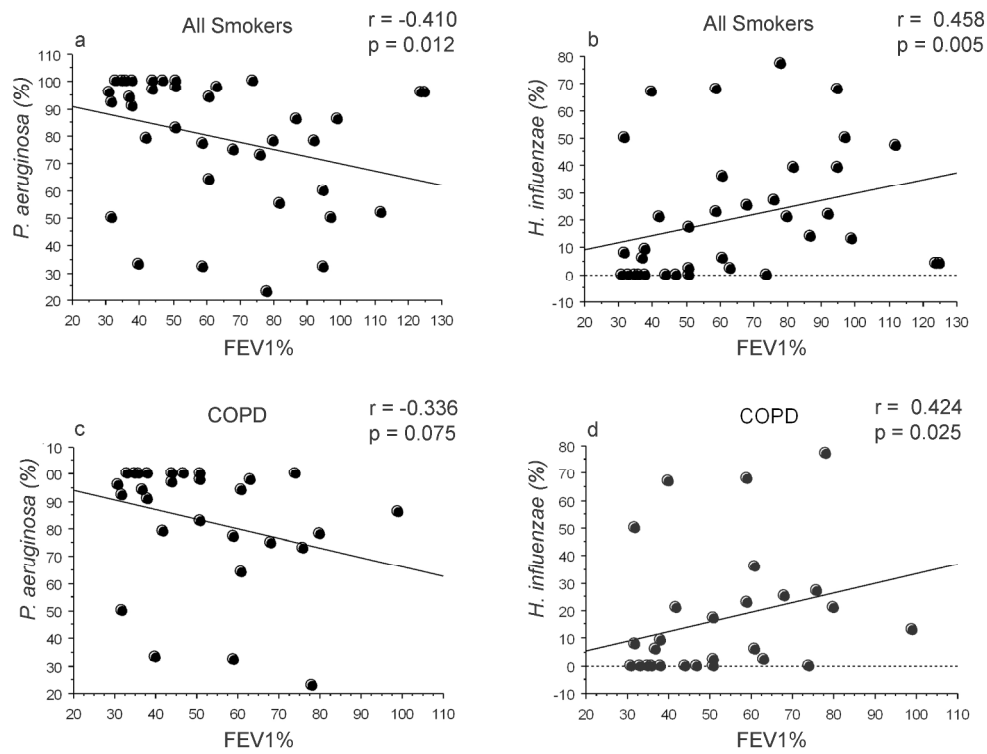
figure 3
figure 3
272x206mm (300 x 300 DPI)

1
2
3
4
5
6
7
8
9
10
11
12
13
14
15
16
17
18
19
20
21
22
23
24
25
26
27
28
29
30
31
32
33
34
35
36
37
38
39
40
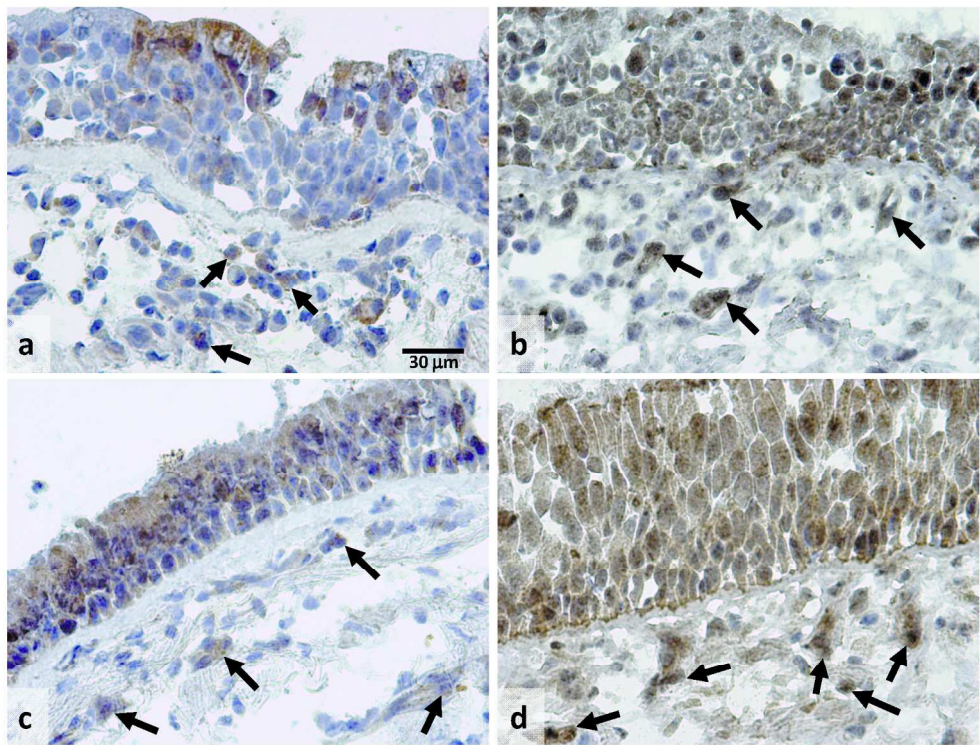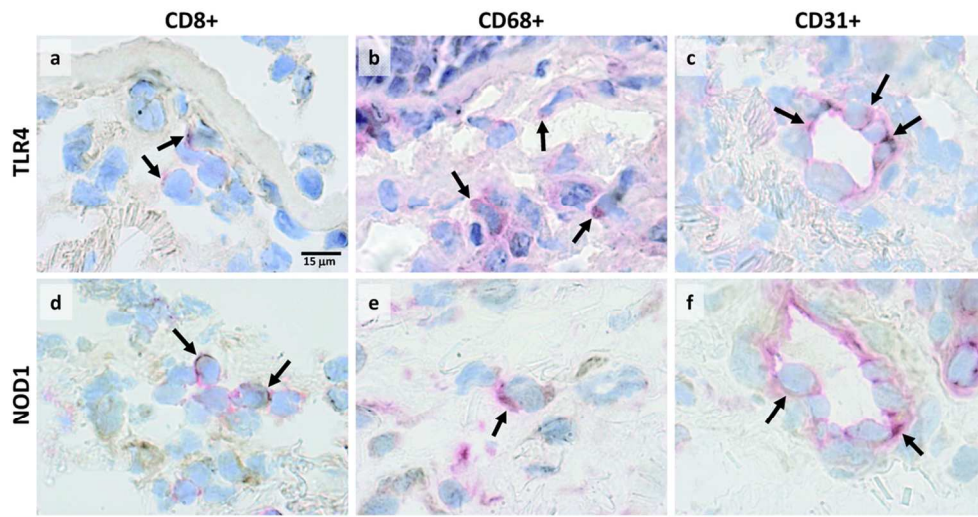41
42
43
44
45
46
47
48
49
50
51
52
53
54
55
56
57
58
59
60
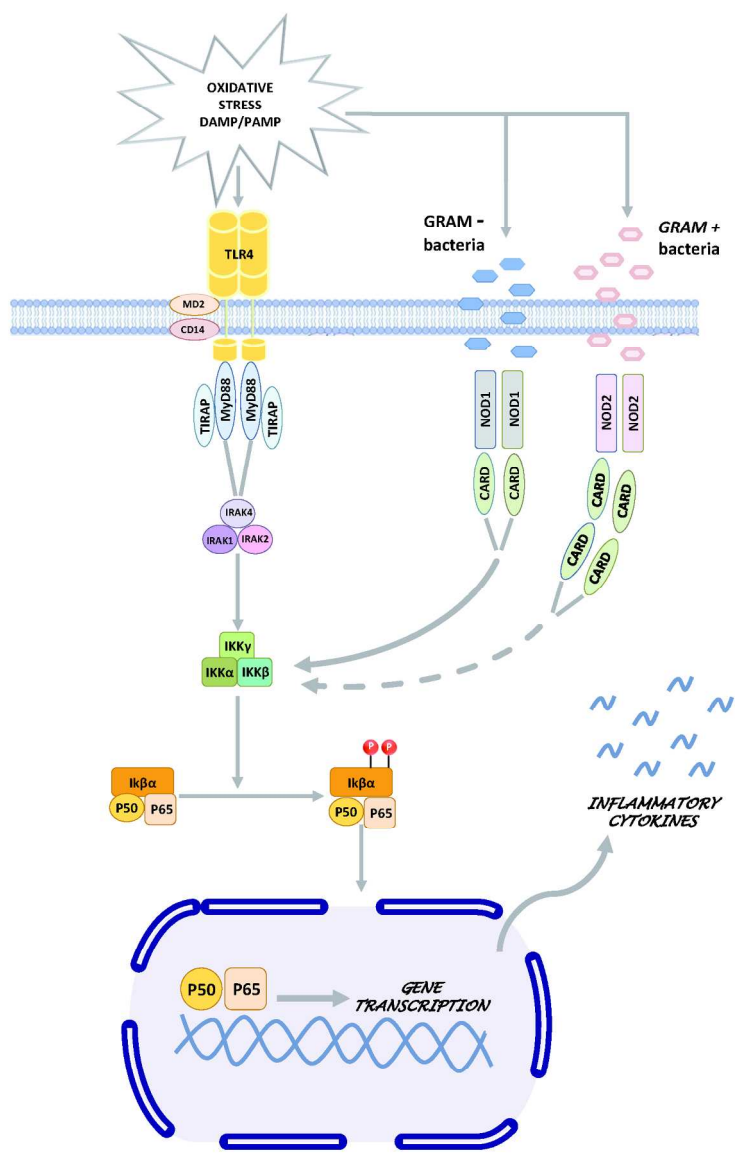
figure 4
figure 4
158x232mm (300 x 300 DPI)
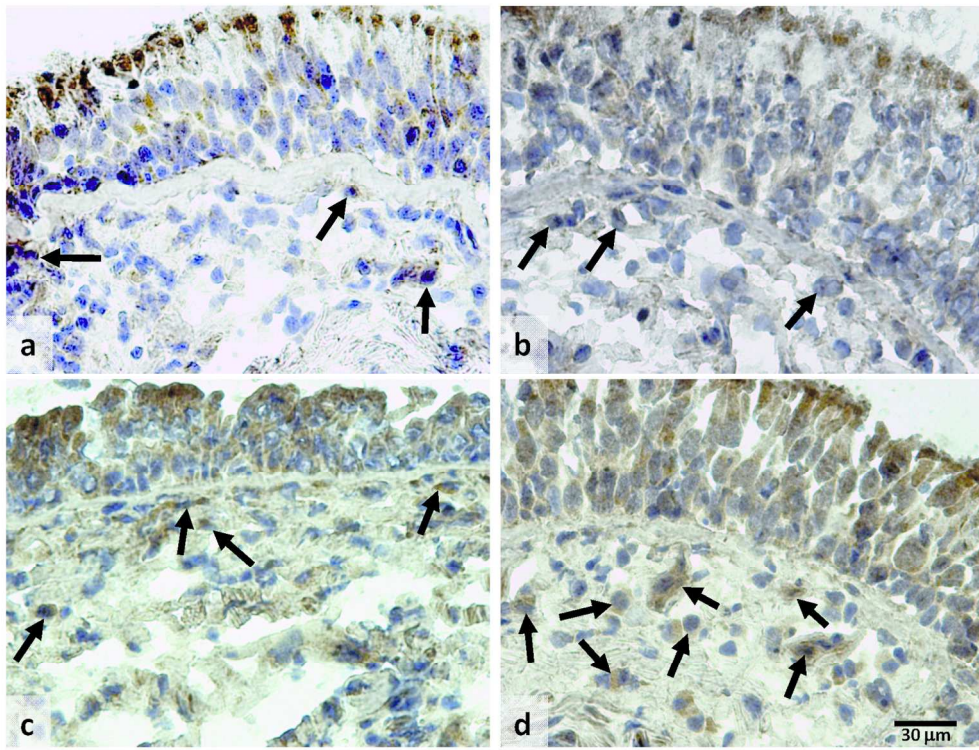
figure E1
figure E1
167x128mm (300 x 300 DPI)

figure E2
figure E2
166x128mm (300 x 300 DPI)

figure E3
figure E3
107x57mm (300 x 300 DPI)